

Accepted Manuscript

Discovery of deshydroxy bicalutamide derivatives as androgen receptor antagonists

Sahar Kandil, Kok Yung Lee, Laurie Davies, Sebastiano A. Rizzo, D. Alwyn Dart, Andrew D. Westwell



PII: S0223-5234(19)30067-4

DOI: <https://doi.org/10.1016/j.ejmech.2019.01.054>

Reference: EJMECH 11061

To appear in: *European Journal of Medicinal Chemistry*

Received Date: 15 November 2018

Revised Date: 9 January 2019

Accepted Date: 22 January 2019

Please cite this article as: S. Kandil, K.Y. Lee, L. Davies, S.A. Rizzo, D.A. Dart, A.D. Westwell, Discovery of deshydroxy bicalutamide derivatives as androgen receptor antagonists, *European Journal of Medicinal Chemistry* (2019), doi: <https://doi.org/10.1016/j.ejmech.2019.01.054>.

This is a PDF file of an unedited manuscript that has been accepted for publication. As a service to our customers we are providing this early version of the manuscript. The manuscript will undergo copyediting, typesetting, and review of the resulting proof before it is published in its final form. Please note that during the production process errors may be discovered which could affect the content, and all legal disclaimers that apply to the journal pertain.

Discovery of deshydroxy bicalutamide derivatives as androgen receptor antagonists

Sahar Kandil^{1*}, Kok Yung Lee¹, Laurie Davies², Sebastiano A. Rizzo¹, D. Alwyn Dart² and Andrew D. Westwell¹

¹School of Pharmacy & Pharmaceutical Sciences, Cardiff University, King Edward VII Avenue, Cardiff, CF10 3NB, Wales, UK. ²Cardiff China Medical Research Collaborative, Cardiff University School of Medicine, Cardiff, CF14 4XN, Wales, UK.

Keywords: Androgen receptor (AR), prostate cancer (PC), castration-resistant prostate cancer (CRPC), bicalutamide, deshydroxy, double branched propioanilide.

Graphical abstract



Highlights

- Synthesis of 23 novel deshydroxy bicalutamide derivatives.
- Identification of novel and potent double branched AR antagonists.
- Enhanced anticancer activity against PC compared to bicalutamide and enzalutamide.
- Strong downregulation of PSA expression in qPCR analysis of LNCaP cell line.
- Molecular modelling provides a rational explanation of the SAR observed.

Abstract

Deshydroxy propioanilides were synthesised by Michael addition reaction between substituted thiophenols onto four different phenylacrylamide derivatives to give twenty-four novel deshydroxy bicalutamide derivatives lacking the central hydroxyl group. The antiproliferative activities of these compounds were evaluated against human prostate cancer cell lines and eleven compounds showed better inhibitory activities (IC₅₀ = 2.67-13.19 μ M) compared to bicalutamide (IC₅₀ = 20.44 μ M) in LNCaP. Remarkably, novel double branched bicalutamide analogues (**27** and **28**) were isolated as major by-products and found to have the best activity across three human prostate cancer cell lines (LNCaP, VCaP and PC3). The most active compound **28** shows sub-micromolar activity (IC₅₀ = 0.43 μ M in LNCaP), which represents more than 40-fold improvement over the clinical anti-androgen bicalutamide (IC₅₀ = 20.44 μ M) and a more than 3 fold improvement over enzalutamide (IC₅₀ = 1.36 μ M). Moreover, strong reduction of PSA expression in LNCaP cells upon treatment with compounds

* Corresponding author
E-mail address: kandils1@cardiff.ac.uk (S. Kandil)

27, 28 and 33 was observed during qPCR analysis, confirming their AR antagonist activity. Molecular modelling studies revealed a novel binding mode of these structurally distinct double branched analogues within the ligand binding domain (LBD) of the androgen receptor.

1. Introduction

The androgen receptor (AR) is expressed in many cell types and plays critical anabolic and reproductive roles in men and women. Androgen receptor (AR) signalling has been found to play crucial functions in modulating tumourigenesis and metastasis in several types of cancers including prostate, bladder, kidney, lung, breast and liver.¹ The initiation and progression throughout the different stages of prostate cancer (PC) is uniquely dependent on the androgen receptor (AR) signalling pathway.^{2,3} Androgen receptor (AR), like other members of the nuclear receptor family, is comprised of three main functional domains: a variable N-terminal domain, a highly conserved DNA-binding domain (DBD) and a conserved ligand binding domain (LBD).⁴ Binding of endogenous hormones; testosterone and dihydrotestosterone (DHT) to the LBD induces conformational changes in the AR that results in its translocation into the nucleus, interaction with DNA, and modulation of specific gene transcription (e.g. prostate specific antigen, PSA).⁵ Androgen receptor antagonists, so-called anti-androgens, are designed to inhibit these processes and are clinically used for the treatment of advanced prostate cancer (PC).^{6,7} Several non-steroidal anti-androgens (NSAA) have been approved for the treatment of PC. The first generation NSAAs include flutamide, hydroxyflutamide, **nilutamide** and bicalutamide (**Figure 1**). They decrease androgenic effects by competitively inhibiting the binding of androgens (testosterone and DHT) to the AR and induce conformational change of H12 via steric clashes. However, these antiandrogens eventually fail to inhibit the AR with the development of castration resistant prostate cancer (CRPC). The development of AR-LBD point mutants (e.g. AR-T877A and AR-W741L) upon long term treatment with NSAAs ultimately result in switching these AR antagonists to AR agonists leading to the relapse of CRPC, which is a more aggressive form of the disease associated with poor prognosis. Similar to the first-generation androgen receptor (AR) antagonists, resistance to the new second generation anti-androgens (enzalutamide, apalutamide) are developing in PC patients, despite the fact that these drugs have better affinity for the AR.⁸ Anti-androgen resistance can also be triggered by the upregulation of the androgen receptor expression, which promotes signalling from low levels of residual hormone.⁸ More recently, darolutamide (ODM-201, **Figure 1**) is under evaluation in phase 3 clinical trials in patients with non-metastatic CRPC.⁹ The discovery of new AR antagonists is urgently needed to improve anti-androgen efficacy and to avoid cross-resistance with the clinically used

compounds.

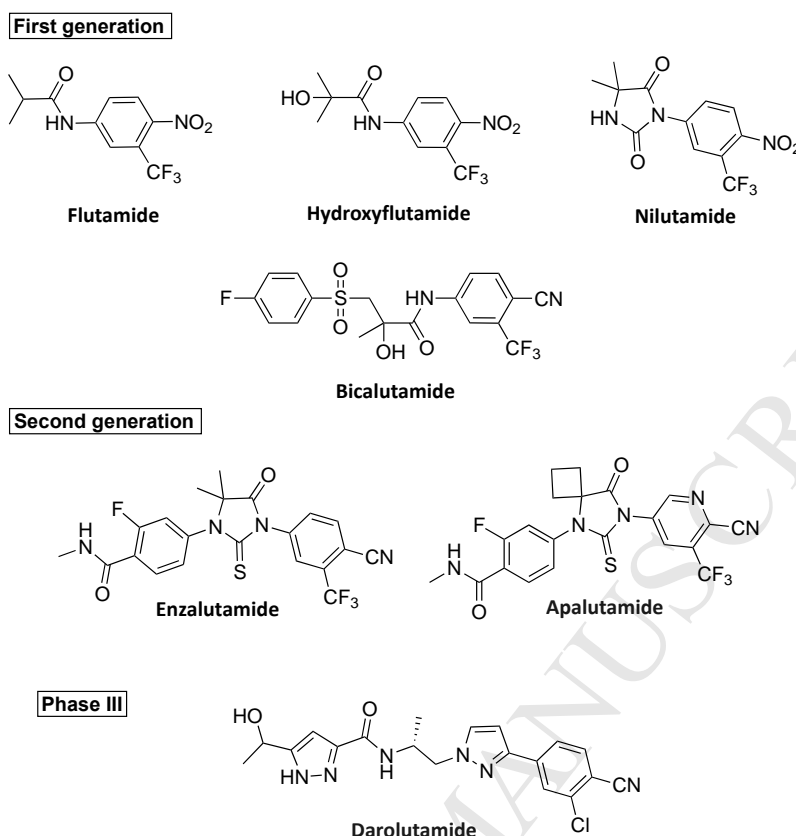


Figure 1. Chemical structures of the non-steroidal anti-androgens (NSAA); flutamide, hydroxyflutamide, nilutamide, and bicalutamide (first generation), enzalutamide and apalutamide (second generation) and darolutamide (phase III clinical trials).

2. Results and discussion

Unfortunately, resistance to clinical anti-androgens has plagued the development of effective therapeutics for advanced prostate cancer (PC). Flutamide and bicalutamide (**Figure 1**) were first generation non-steroidal AR antagonists. However, these antiandrogens lose their activity with time upon the development of AR-LBD point mutants (AR-T877A and AR-W741L) triggered by flutamide and bicalutamide, respectively. On the other hand, AR-F876L mutation causes enzalutamide and apalutamide (ARN-509) to function as AR agonists and confers drug resistance across multiple AR models both *in vitro* and *in vivo*.¹⁰ The X-ray structure of bicalutamide inside the LBD site of the AR - W741L mutant, (PDB 1Z95), provides a significant insight into the protein-drug interactions and explains the structural basis for the conversion of bicalutamide from AR antagonist into AR agonist.¹⁰
¹¹ The binding mode of bicalutamide as an antagonist of the AR-wild type compared to its binding mode as an agonist of the AR-W741L mutant is shown in **Figure 2**. It is observed that helix 12 (H12) has changed its position from an open antagonist conformation (AR- wild type, blue) to a closed

agonist conformation (AR- W741L mutant, green). In the case of the antagonist mode, ring B of bicalutamide is pointing outwards away from Trp⁷⁴¹ and towards helix 12, thus preventing AR from adapting the closed AR agonist conformation. The loss of the steric bulk of the indolyl side chain of tryptophan⁷⁴¹ to the smaller size side chain of Leucine⁷⁴¹ lead to the elimination of the steric clash and hence the incorporation of bicalutamide molecule into the closed activated conformation of AR.

10-12

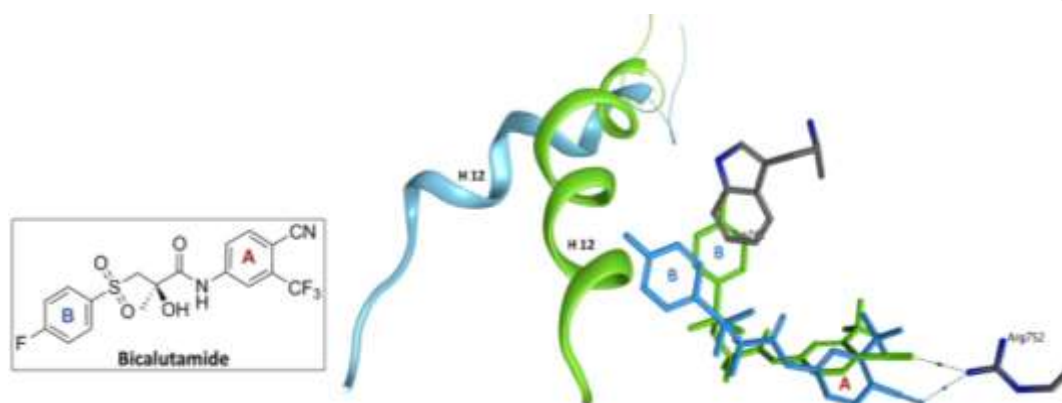


Figure 2. Proposed structural basis for the conversion of bicalutamide from AR antagonist into AR agonist by the gain-of-function mutation (W741L); the X-ray structure of bicalutamide (green) inside the closed agonist conformation of AR LBD-W741L, (green, PDB 1Z95) compared to its binding mode (blue) inside the open antagonist conformation of AR LBD-wt, showing ring B orientation to hinder helix 12 from closing to an agonist conformation.

From previous studies, we have learnt that the size and structure of ring B determine the activity of the anti-androgen and if possesses the correct volume and orientation, it will prevent the anti-androgen molecule from being completely confined in the AR-LBD pocket cavity, leaving its bulky substituents protruding against helix 12 (H12) and stopping the latter from adopting a position essential for coactivator interaction (agonist closed conformation).¹⁰⁻¹²

Previously, we have found that the introduction of 3,5-*bis*-trifluoromethyl (3,5-*bis*-CF₃) substituents into ring B of bicalutamide, enobosarm and umbelliferone derivatives, has profoundly modified their anti-proliferative activity, pharmacokinetic and tissue distribution profiles by providing the geometric bulk needed to keep ring B towards Helix 12 while keeping the crucial interactions of the nitrile/nitro group of ring A with Arg 752.¹³⁻¹⁵ Noting that both flutamide and darolutamide (ODM-201) are lacking the linker OH group, **Figure 1**, in this work we studied whether the central hydroxyl group of bicalutamide is necessary for maintaining the anti-androgen activity and if the successive increase in the bulk size of ring B substituents (from 4-F → 4-CF₃ → 3,5-*bis*-CF₃) would compensate for the smaller size of the deshydroxy linker (lacking the central OH group). We used four different variations of aromatic ring A (**Figure 3**); all containing the necessary 4-CN or 4-NO₂ for the interaction with Arg

752 in addition to either 2-CF₃ or 3-CF₃ substituent to understand better the structure activity relationship.

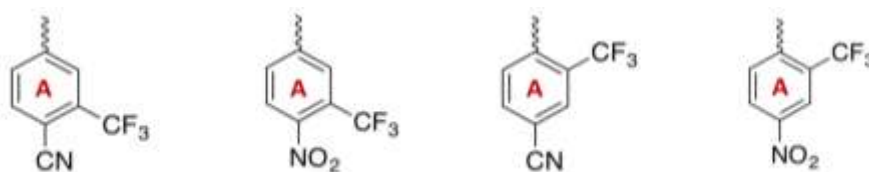
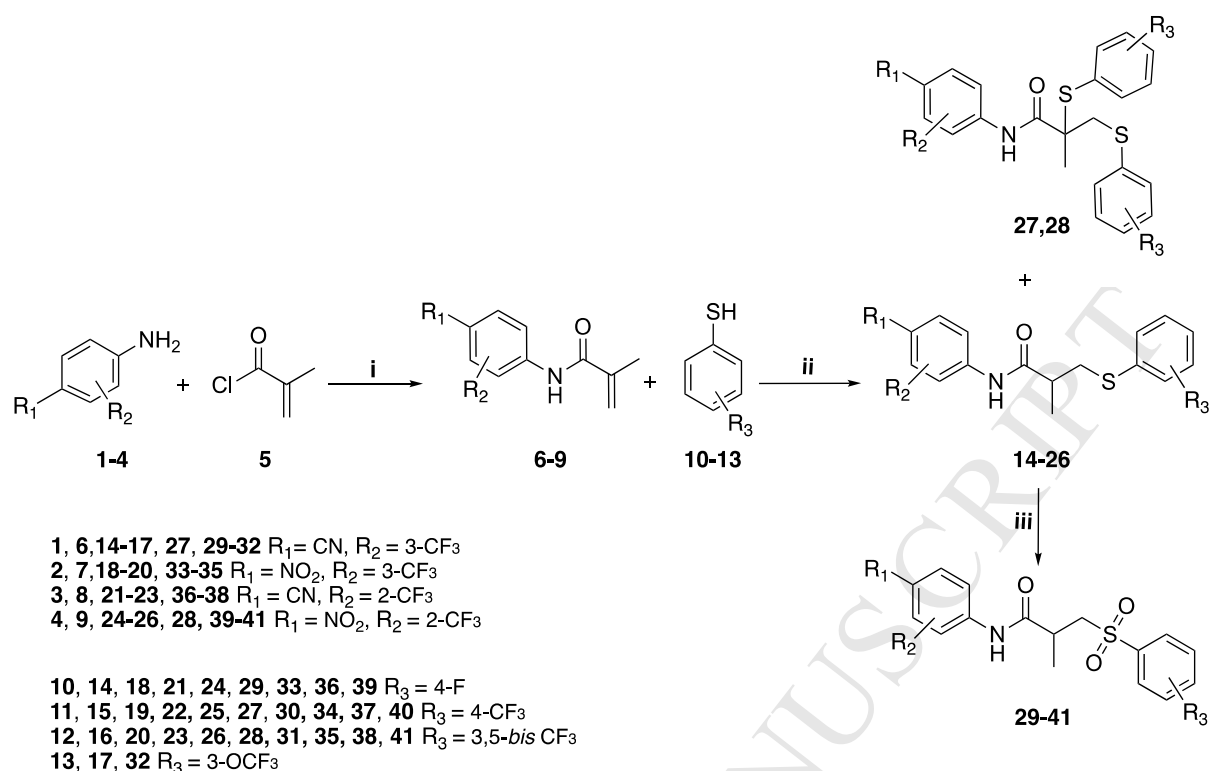


Figure 3. Four different variations of ring A containing 4-CN or 4-NO₂ group in addition to either 2-CF₃ or 3-CF₃

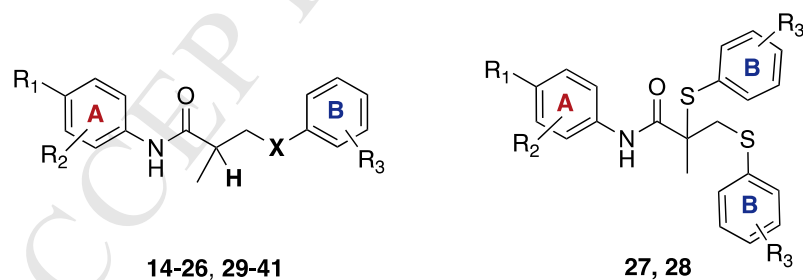
2.1 Chemistry

The novel series of deshydroxy propioanilide analogues (**29-41**) were synthesised in three steps. An acylation reaction between the corresponding substituted trifluoromethyl anilines (**1-4**) with methacryloyl chloride (**5**) in dimethylacetamide (DMA) to obtain phenylmethacrylamide derivatives (**6-9**)^{16,17} was followed by Michael addition of the corresponding substituted thiophenols (**10-13**) to obtain the thioether intermediates (**14-26**, 19-56% yield), which were subsequently oxidised to the corresponding sulfone derivatives (**29-41**, 19-95% yield) using 3-chloroperbenzoic acid (*m*CPBA) (**Scheme 1**). It is worth noting that the thioethers (**14-20** and **24-26**) were prepared using sodium hydride (NaH) in tetrahydrofuran (THF) at room temperature (method A), whereas the thioethers (**21-23**) corresponding to the *N*-(4-cyano-2-(trifluoromethyl)phenyl) methacrylamide (**8**) were prepared using aqueous sodium hydroxide solution and tetrabutylammonium chloride in 1,4-dioxane and reflux for 3 hours instead (method B), as the first method did not yield any products.¹⁸ The intermediate sulphides (**15**, **16**, **20-22**) were used directly into the next oxidation step since further purification was not feasible. Interestingly, alongside the thioether compounds (**15** and **26**) we obtained two unusual disubstituted (double branched) acrylamide derivatives (**27** and **28**, respectively) as major by-products in an approximate ratio of 2 (double branched **27** and **28**) : 1 (single branched **15**, **26**), **scheme 1**.



Scheme 1. Synthesis of racemic deshydroxy propioanilide derivatives. Reagents and conditions: (i) methacryloyl chloride **5** (8 equiv), DMA, rt, 3 h; (ii) thiophenol derivatives (**10-13**, 1.2 equiv), method A: NaH (1.2 equiv), THF, rt, 24 h (**6,7,9**) or method B: NaOH, 1,4-dioxane, tetrabutylammonium chloride reflux 3 hr (**8**); (iii) mCPBA (1.4 equiv), DCM, rt, 4-6 h.

The mechanism of the formation of the double branched products remains to be fully clarified. All compounds were purified by column chromatography and/or recrystallised. The structures of all the synthesised compounds were confirmed using analytical and spectroscopic data (^1H NMR, ^{13}C NMR, ^{19}F NMR and mass spectrometry), which were in full accordance with their depicted structures.



ID	R_1	R_2	R_3	X	IC_{50} (uM)
14	CN	3- CF_3	4-F	S	8.69
15	CN	3- CF_3	4- CF_3	S	-
16	CN	3- CF_3	3,5-Bis CF_3	S	-
17	CN	3- CF_3	3- OCF_3	S	114.97
18	NO_2	3- CF_3	4-F	S	27.16
19	NO_2	3- CF_3	4- CF_3	S	4.41
20	NO_2	3- CF_3	3,5-Bis CF_3	S	-
21	CN	2- CF_3	4-F	S	-
22	CN	2- CF_3	4- CF_3	S	-
23	CN	2- CF_3	3,5-Bis CF_3	S	4.57
24	NO_2	2- CF_3	4-F	S	43.19

25	NO ₂	2-CF ₃	4-CF ₃	S	54.33
26	NO ₂	2-CF ₃	3,5-BisCF ₃	S	43.68
27	CN	3-CF ₃	4-CF ₃	-	1.68
28	NO ₂	2-CF ₃	3,5-BisCF ₃	-	0.43
29	CN	3-CF ₃	4-F	SO ₂	114.74
30	CN	3-CF ₃	4-CF ₃	SO ₂	57.98
31	CN	3-CF ₃	3,5-BisCF ₃	SO ₂	6.16
32	CN	3-CF ₃	3-OCF ₃	SO ₂	13.19
33	NO ₂	3-CF ₃	4-F	SO ₂	2.67
34	NO ₂	3-CF ₃	4-CF ₃	SO ₂	3.31
35	NO ₂	3-CF ₃	3,5-BisCF ₃	SO ₂	12.23
36	CN	2-CF ₃	4-F	SO ₂	137.7
37	CN	2-CF ₃	4-CF ₃	SO ₂	28.79
38	CN	2-CF ₃	3,5-BisCF ₃	SO ₂	9.56
39	NO ₂	2-CF ₃	4-F	SO ₂	4.05
40	NO ₂	2-CF ₃	4-CF ₃	SO ₂	26.34
41	NO ₂	2-CF ₃	3,5-BisCF ₃	SO ₂	3.08
Bical	-	-	-	-	20.44
Enzal	-	-	-	-	1.31

Table 1. Chemical structure and *in vitro* anti-proliferative activity (IC₅₀ in μ M) of single (**14-26**, **29-41**) and double (**27**, **28**) branched deshydroxy propioanilide analogues compared to bicalutamide and enzalutamide in the LNCaP cell line. IC₅₀ values presented are the mean of three independent experiments.

2.2 Cell growth inhibition activity

The twenty-four novel deshydroxy antiandrogen compounds **14**, **17-19**, **23-41**, were tested for their anti-cancer activity as racemic mixtures against human androgen-sensitive prostate cancer cell line LNCaP at 9 concentrations in half-log increments up to 100 μ M for 96 hours in triplicate. Bicalutamide and enzalutamide were used as positive controls. Potency is expressed as absolute IC₅₀ values, calculated by non-linear regression analysis. The results summarised in **Table 1** indicated that thirteen compounds (**14**, **19**, **23**, **27**, **28**, **31-35**, **38**, **39** and **41**) showed better anti-proliferative activity than bicalutamide with IC₅₀ values in the range of 0.43-13.19 μ M, while the positive controls, bicalutamide and enzalutamide exhibited IC₅₀ values of 20.44 and 1.31 μ M, respectively. Interestingly, the double branched compounds **27** and **28** exhibited significantly potent activity compared to bicalutamide and enzalutamide in LNCaP cell line (**Table 2**). The most active compounds **27**, **28** and **33** (**Figure 4**) were selected to be further tested against VCaP and PC3 human prostate cancer cell lines, which represent metastatic and more aggressive forms of prostate cancer (CRPC).¹⁹

Compound ID	LNCaP IC ₅₀ (μ M)	VCaP IC ₅₀ (μ M)	PC3 IC ₅₀ (μ M)
27	1.68	0.13	5.45
28	0.43	0.18	0.91
33	2.67	8.21	112.30
Bicalutamide	20.44	5.96	92.63
Enzalutamide	1.31	3.66	15.07

Table 2. *In vitro* anti-proliferative activity (IC₅₀ in μ M) of compounds (**33**, **27** and **28**) compared to bicalutamide and enzalutamide in human prostate cancer cell lines; LNCaP, VCaP and PC3

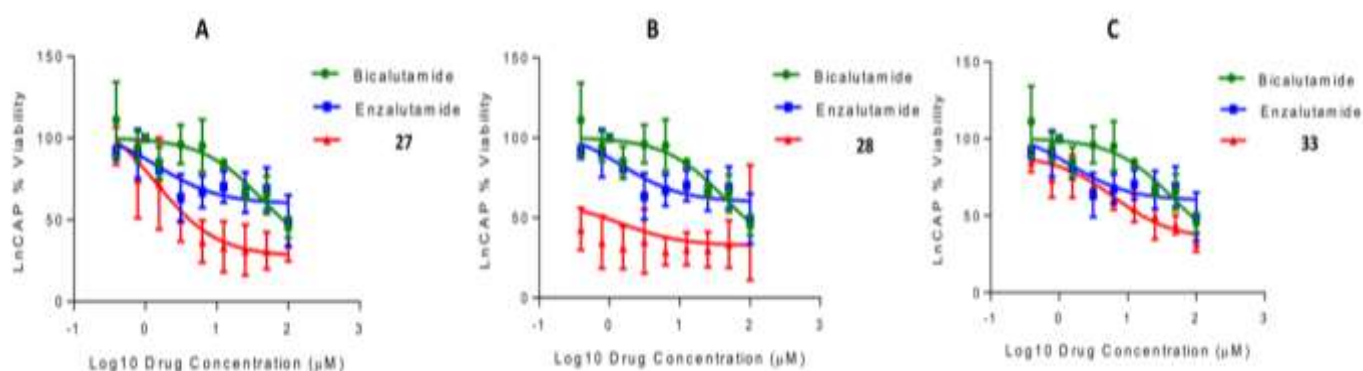


Figure 4. Dose-response relationship of LNCaP cells treated with 0-100 μM of compounds; (**27**, **A**), (**29**, **B**) or (**33**, **C**) (red), bicalutamide (green) and enzalutamide (blue) for 96 h. Data is presented as the mean \pm SD of three replicates at each concentration.

2.3 Downregulation of PSA Expression in LNCaP Cells

Prostate specific antigen (PSA) is a serine protease that is synthesised by both normal and malignant epithelial cells of the human prostate. The expression of PSA is mainly induced by androgens and regulated primarily by the androgen receptor (AR) at the transcriptional level^{20,21}. The effect of compounds **27**, **28** and **33** on prostate specific antigen (PSA, an AR-regulated gene) expression was analysed using qPCR after incubation of LNCaP cells with 5, 10, 50 and 100 μM of bicalutamide, compounds **27**, **28** and **33**, for 24-hours. The analysis shows that the three compounds **27**, **28** and **33** exhibited dose dependent inhibition of PSA expression with compound **28** showing the best activity significantly exceeding that of bicalutamide (**Figure 5**). The significant reduction of the AR-regulated PSA expression in the qPCR analysis, suggests that these compounds have strong AR-antagonist activity.

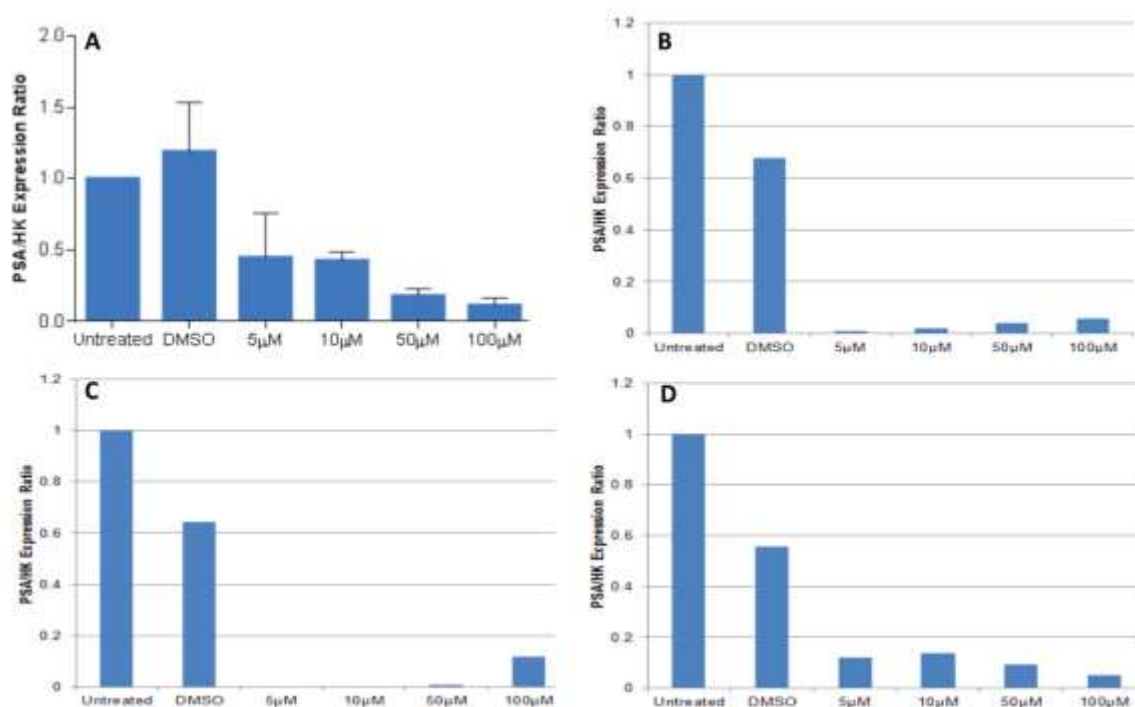


Figure 5. The relative change in PSA expression (PSA/HK) in LNCaP cells upon treatment with increasing doses of bicalutamide (A), compounds; **27** (B), **28** (C) and **33** (D). HK: housekeeping genes (Bactin and GAPDH)

2.4 Docking studies reveal a structural basis for anti-androgen activity

Previous X-ray crystallographic studies of androgen receptor have elucidated the structures of the AR ligand binding domain (LBD) bound to agonists, and of mutant AR bound to antagonists in an agonist like conformation. However, there are no crystal structures of the AR-LBD in an antagonist conformation reported so far.^{22,23} The human progesterone receptor (hPR residues 683-931) has 56% primary sequence homology to the hAR (residues 669-918) and 32% of these residues are conservative mutations, giving an overall sequence homology of 87%.²⁴ Building on this information, the hPR crystal structure [PDB 2OVH]²⁵ was used as a template to build an hAR homology model (HM) using the sequence of the hAR in the agonist conformation [PDB 2AMA].²⁶ Applying the default parameters of MOE (Molecular Operating Environment - Chemical Computing Group, Montreal, Canada) homology modelling module and using the AMBER99 force field, a total of 10 homology models were generated. The quality of each model was assessed within MOE, and the best model was chosen for the docking studies.

Computational docking studies were performed to explore the binding modes of the deshydroxy propioanilide analogues (**14-41**) within the AR-LBD binding site. The chemical structures of our compounds (**14-41**) were constructed, rendered and minimized with the MMFF94x force field in MOE. Docking simulations were performed using Glide SP in Maestro (Glide, version 9.5, Schrödinger,

LLC, New York, NY. <http://www.schrodinger.com>). The putative docking modes of the most active single branched deshydroxy propioanilide compounds **41**, **34** and **33** (IC_{50} = 3.08, 3.31 and 2.67 μ M, respectively) are shown in **Figure 6** (A-C, respectively). All three compounds show the crucial H-bond interaction between their nitro group (4-NO₂, ring A) and the guanidine group of the Arg-752 residue. Other key interactions of compound **41** include an H-bond between the aromatic ring B (ArH) and carbonyl group of Asn 705 and the carbonyl group and Met 742 (Figure 5A). Compound **34** shows an additional H-bond between the nitro group (4-NO₂, ring A) and the amino group of Gln 711, and another H-bond between the amide NH group and the carbonyl group of Leu 704. Also, a H-bond between the sulphone group and the side chain of Met 745 residue was observed (Figure 5B). Compound **33** shows a hydrogen bond between the aromatic ring A and the side chain of Met 742 residue, and another H-bond between the sulphone group and the side chain of Met 745 residue.

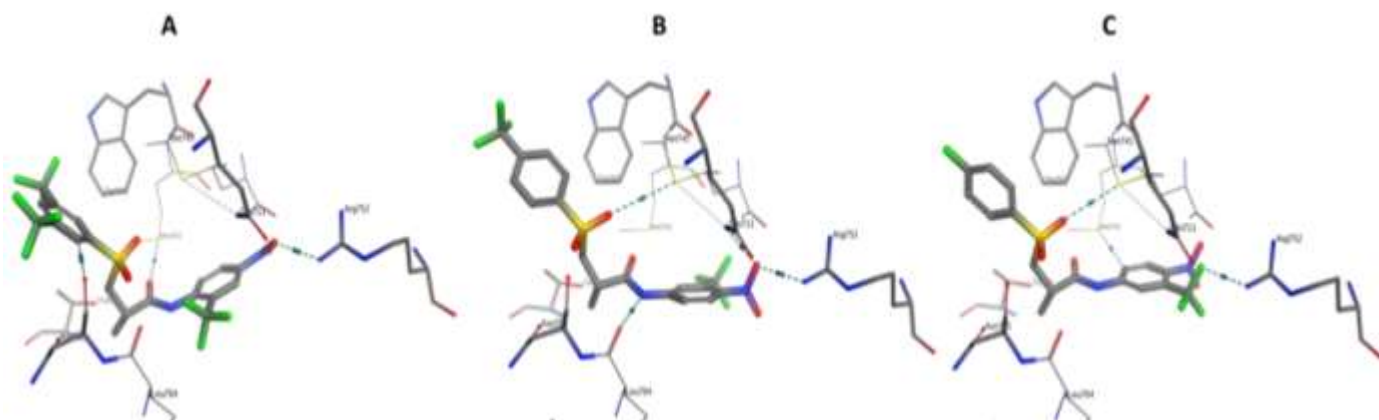


Figure 6. The predicted binding modes of compounds (**41**, A), (**34**, B) and (**33**, C) inside the hAR-LBD showing H-bond interactions with key amino acids; Arg752, Gln711, Met 742, Met 745, Leu704, Thr877 and Asn705.

On the other hand, the docking of the double branched deshydroxy compounds (**27** and **28**) revealed an interesting binding mode where the ring A aryl nitrile (4-CN, **27**) and aryl nitro (4-NO₂, **28**) groups form a hydrogen bond with the guanidine group of Arg752 in the AR ligand binding pocket, mimicking the interaction between the 3-keto functionality of the hormone dihydrotestosterone (DHT) and the androgen receptor. The two branches of ring B occupy simultaneously the two sub-pockets that are known to be involved in the binding of bicalutamide and enzalutamide²⁷ which may explain well the high potency observed with this type of distinctive scaffold (**Figure 7**).

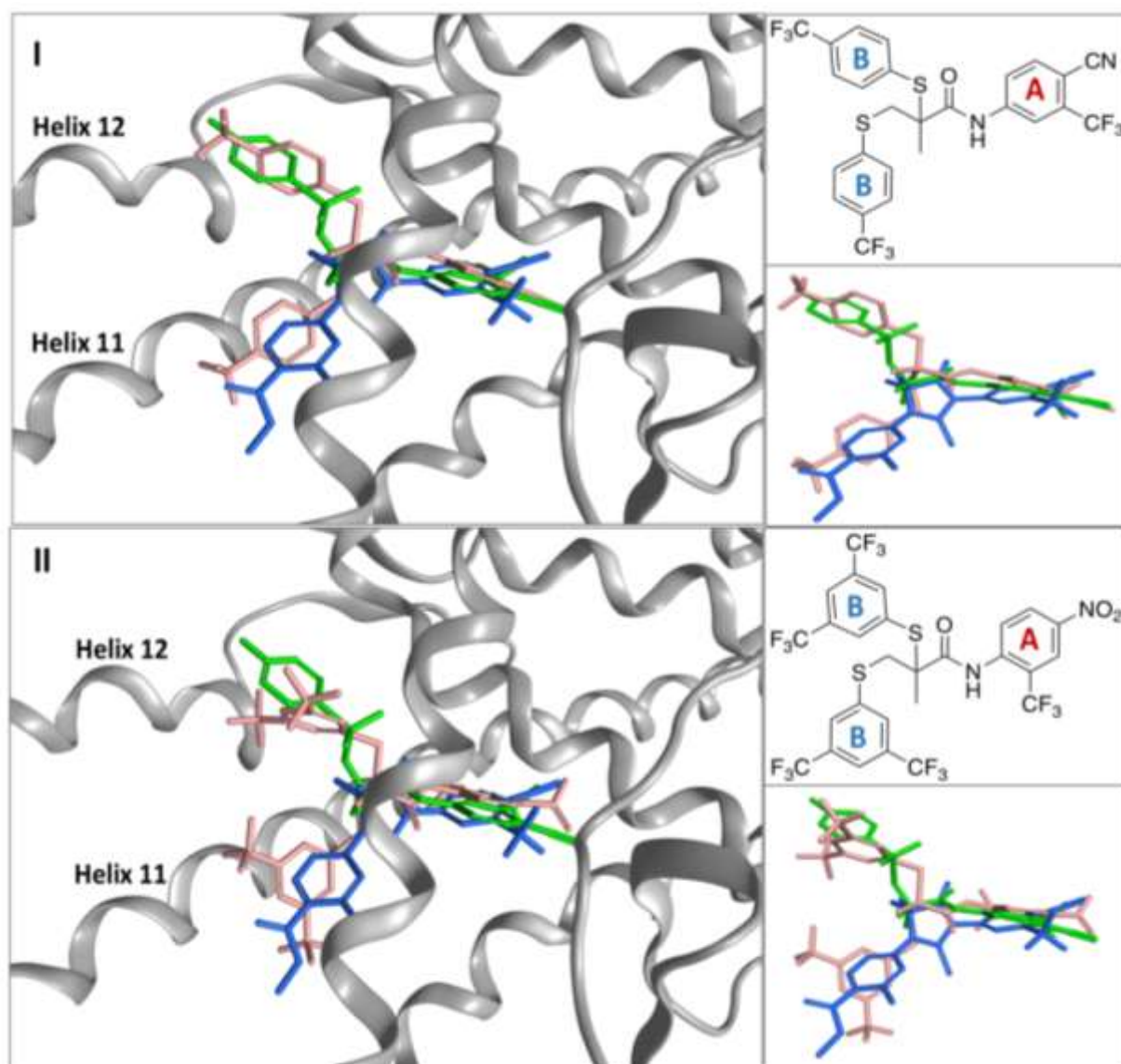


Figure 7. The predicted binding modes of bicalutamide (green), enzalutamide (blue) compared to the double-branched compounds (pink); **27** (I) and **28** (II) within the hAR-LBD (grey ribbon). Left panel (top) is showing the 2D representation of compound **27** (I) and compound **28** (II).

Generally, our SAR analysis of this family of compounds indicates that the lack of the linker hydroxy group of the propionanilide scaffold seems to be tolerated in terms of the anti-proliferative activity in PC cell lines and in some cases showed enhanced activity compared to bicalutamide; compounds (**14**, **19**, **23**, **27**, **28**, **31-35**, **38**, **39** and **41**). Compounds **27** and **28** were significantly more potent than both bicalutamide and enzalutamide in our models. Docking studies suggest that this enhanced activity can be attributed to the steric bulk added by the two branches of the aromatic ring B which occupy both the proposed binding pockets of bicalutamide and enzalutamide simultaneously and would provide the geometric bulk needed to keep ring B pointing outwards away from Trp⁷⁴¹ and towards helix 12, thus preventing AR from adapting the AR agonist (closed) conformation (**Figure 7**). These

double branched compounds (**27** and **28**) are distinct from the structures of other nonsteroidal anti-androgens, which is likely to result in differences in biology and resistance mechanisms.

3. Conclusion

A series of twenty-four novel deshydroxy bicalutamide analogues (**29-41**) were synthesised using a Michael addition reaction between four different acrylamide derivatives (**6-9**) and various fluorinated thiophenols (**10-13**) as a key step. Eleven compounds showed anti-proliferative activity (IC_{50} = 0.43-13.19 μ M) better than bicalutamide (IC_{50} = 20.44 μ M). Interestingly, compounds **27** and **28** exhibited very potent activity with IC_{50} values of 1.68 and 0.43 μ M, respectively, which is comparable or better than enzalutamide (IC_{50} = 1.31 μ M) in the LNCaP cell line. Further testing for the *in vitro* anti-proliferative activity in VCaP and PC3 cell lines showed sub-micromolar activity. Furthermore, compounds **27**, **28** and **33** showed remarkable reduction of PSA expression in LNCaP cells confirming their anti-androgenic activity. Molecular modelling studies indicated that the enhanced anti-androgen activity of compounds **27** and **28** appears to be a result of the extra bulk conferred by the two aromatic rings B, which ensure the occupation of the two sub-pockets of the AR-LBD involved in the binding interaction of bicalutamide and enzalutamide simultaneously. This may forestall the drug resistance seen with current clinical anti-androgens. Compounds **27** and **28** have distinctive chemical structure and represents promising lead for further development of AR antagonists. Overall, this study provides, for the first time, the double-branched configuration into the non-steroidal anti-androgen library and lays a foundation for the development of alternative AR antagonist therapies capable of combating prostate cancer.

Acknowledgment

The authors would like to thank the Welsh Government (A4B-Academic Expertise for Business), the Life Sciences Research Network of Wales (LSRNW), and the Cardiff China Medical Research Collaborative. We also thank the EPSRC National Mass Spectrometry centre (Swansea, U.K.) for provision of accurate mass spectrometry.

Supplementary data

1H , ^{19}F and ^{13}C NMR spectra, and mass spectrometry data, for representative compounds **25**, **28**, and

35

4. Experimental section

4.1 Chemistry

All chemicals were purchased from Sigma-Aldrich or Alfa Aesar and were used without further

purification. Thin Layer Chromatography (TLC): pre-coated aluminium backed plates (60 F₂₅₄, 0.2 mm thickness, Merck) were visualized under both short and long wave UV light (254 and 366 nm). Flash column chromatography was carried out using silica gel supplied by Fisher (60A, 35-70 μ m). ¹H NMR (500 MHz), ¹³C NMR (125 MHz) and ¹⁹F NMR (470 MHz) spectra were recorded on a Bruker Avance 500 MHz spectrometer at 25° C. Chemical shifts (δ) are expressed in parts per million (ppm) and coupling constants (J) are given in hertz (Hz). The following abbreviations are used in the assignment of NMR signals: s (singlet), bs (broad singlet); d (doublet), t (triplet), q (quartet), qn (quintet), m (multiplet), dd (doublet of doublet), dt (doublet of triplet), td (triple doublet); dq (double quartet), m (multiplet), dm (double multiplet). Mass spectrometry was performed as a service through the EPSRC National Mass Spectrometry centre (Swansea, UK).

4.1.1 General method for the preparation of intermediates 6-9

Methacryloyl chloride **5** (8.4 mL, 85.96 mmol) was added over the course of 10 minutes to a stirring solution of the appropriate trifluoromethyl-substituted aniline **1-4** (10.75 mmol) in N, N-dimethylacetamide (10 mL) at room temperature for 24h. After the reaction was complete, the mixture was diluted with ethyl acetate (100 mL), extracted with saturated NaHCO₃ solution (2 x 50 mL) then cold brine (2 x 50 mL). The combined organic layer was dried over anhydrous Na₂SO₄ and the solvent was removed under reduced pressure. The crude oil residue was purified by flash column chromatography eluting with chloroform-ethyl acetate 95:5 v/v to obtain the titled compounds.

N-(4-cyano-3-(trifluoromethyl)phenyl)methacrylamide (6)¹⁶. Yield; 92%

¹H NMR (CDCl₃) δ 8.10 (d, *J* = 2 Hz, 1H, ArH), 8.06 (bs, 1H, NH), 8.01 (dd, *J* = 2, 8.5 Hz, 1H, ArH), 7.81 (d, *J* = 8.5 Hz, 1H, ArH), 5.89 (d, *J* = 1 Hz, 1H, CH₂), 5.62 (q, *J* = 1.5 Hz, 1H, CH₂), 2.10 (dd, *J* = 0.5, 1.5 Hz, 3H, CH₃). ¹⁹F-NMR: (CDCl₃) δ -62.23.

N-(4-nitro-3-(trifluoromethyl)phenyl)methacrylamide (7)¹⁶. Yield; 80%

¹H-NMR (CDCl₃): δ 7.99-7.95 (m, 2H, ArH), 7.93 (d, *J* = 9 Hz, 1H, ArH), 7.8 (bs, 1H, NH), 5.81 (q, *J* = 1 Hz, 1H, CH₂), 5.55 (q, *J* = 1.5 Hz, 1H, CH₂), 2.02 (dd, *J* = 1, 1.5 Hz, 3H, CH₃). ¹⁹F-NMR (CDCl₃): δ -60.09.

N-(4-cyano-2-(trifluoromethyl)phenyl)methacrylamide (8)¹⁷. Yield; 88 %

¹H-NMR (CDCl₃): δ 8.69 (d, *J* = 9 Hz, 1H, ArH), 8.07 (bs, 1H, NH), 7.84 (d, *J* = 1.5 Hz, 1H, ArH), 7.78 (dd, *J* = 2, 9 Hz, 2 Hz, 1H, ArH), 5.83 (q, *J* = 1 Hz, 1H, CH₂), 5.56 (q, *J* = 1.5 Hz, 1H, CH₂), 2.02 (dd, *J* = 1, 1.5 Hz, 3H, CH₃). ¹⁹F-NMR (CDCl₃): δ -61.35.

N-(4-nitro-2-(trifluoromethyl)phenyl)methacrylamide (9)¹⁷ Yield; 94 %

^1H NMR (CDCl_3) δ 8.73 (d, J = 9 Hz, 1H, ArH), 8.46 (d, J = 3 Hz, 1H, ArH), 8.37 (dd, J = 9 Hz, 2.5 Hz, 1H, ArH), 8.17 (bs, 1H, NH), 5.85 (q, J = 0.5 Hz, 1H, CH_2), 5.58 (q, J = 1.5 Hz, 1H, CH_2), 2.15-2.13 (dd, J = 1, 1.5 Hz, 1H, CH_3). ^{19}F -NMR: (CDCl_3) δ -61.31.

4.1.2 General method for the preparation of sulphide intermediates;

4.1.2.1 Method A: (14-20 and 24-28)

To a mixture of 60% sodium hydride in mineral oil (94.43 mg, 2.36 mmol) in anhydrous tetrahydrofuran (5 mL) at 0°C under anhydrous THF under nitrogen atmosphere, was added dropwise the corresponding thiophenol **10-13** (2.05 mmol). This mixture was stirred at room temperature for 20 minutes. A solution of the appropriate intermediate **6-9** (1.57 mmol in 5 mL anhydrous tetrahydrofuran) was added slowly to the thiophenol mixture and stirred at room temperature for 24h. The mixture was concentrated under vacuum then diluted with ethyl acetate (30 mL), washed with brine (20 mL) and water (30 mL), dried over anhydrous sodium sulfate and concentrated under vacuum. The crude residue was purified by column chromatography eluting with chloroform-ethyl acetate gradually increasing from 95:5 to 90:10 v/v.

4.1.2.2 Method B: (21-23)

The corresponding thiophenol **10-13** (2.05 mmol) was added dropwise to an aqueous sodium hydroxide solution (79 mg in 1 mL water) for 15 min at room temperature. Then a solution of compound **8** (2.05 mmol) in 1,4-dioxane (5 mL) was added at room temperature followed by a catalytic amount of tetrabutylammonium bromide. The reaction mixture was refluxed for 3 h and cooled to room temperature, followed by addition of 26% aqueous acetic acid. This mixture was extracted with ethyl acetate (2 x 200 mL). The ethyl acetate layer was separated, washed with water, and concentrated under reduced pressure. The crude residue was purified by column chromatography eluting with chloroform-ethyl acetate gradually increasing from 95:5 to 90:10 v/v.

***N*-(4-cyano-3-(trifluoromethyl)phenyl)-3-((4-fluorophenyl)thio)-2-methylpropanamide (14)**. Yield; 50%

^1H -NMR: (CDCl_3) δ 8.01 (s, 1H, ArH), 7.90 (d, J = 8.5 Hz, 1H, ArH), 7.85 (s, 1H, NH), 7.79 (d, J = 9 Hz, 1H, ArH), 7.38 (dd, J = 5.5, 8 Hz, 2H ArH), 7.00 (t, J = 8.5 Hz, 2H, ArH), 3.28 (dd, J = 8, 14 Hz, 1H, CH_2), 3.04 (dd, J = 5, 13.5 Hz, 1H, CH_2), 2.64 (sext, J = 7 Hz, 1H, CH), 1.37 (d, J = 7 Hz, 3H, CH_3). ^{19}F -NMR: (CDCl_3) δ -62.23, -114.26, ^{13}C -NMR: (CDCl_3) δ 173.59 (C=O), 162.04 (d, $^1J_{\text{C-F}}$ = 246.4 Hz, ArC), 142.10 (ArC), 135.79 (ArCH), 133.99 (q, $^2J_{\text{C-F}}$ = 32.9 Hz, ArC), 132.64 (d, $^3J_{\text{C-F}}$ = 8 Hz, ArCH), 130.04 (d, $^4J_{\text{C-F}}$ = 3.6 Hz, ArC), 122.10 (q, $^1J_{\text{C-F}}$ = 272.5 Hz, CF_3), 121.85 (ArCH), 117.31 (q, $^3J_{\text{C-F}}$ = 4.6 Hz, ArCH), 116.32 (d, $^2J_{\text{C-F}}$ = 21.8 Hz,

ArCH), 115.63 (CN), 104.08 (ArC), 42.62 (CH), 38.57 (CH₂), 17.66 (CH₃). HRMS calcd for C₁₈H₁₄F₄N₂OS [M+H], 383.0836; found, 383.0836.

***N*-(4-cyano-3-(trifluoromethyl)phenyl)-2-methyl-3-((3-(trifluoromethoxy)phenyl)thio) propanamide (17).** Yield; 47%

¹H-NMR: (CDCl₃) δ 8.54 (s, 1H, NH), 8.08 (d, *J* = 1.5Hz, 1H, ArH), 7.94 (dd, *J* = 2, 8.5Hz, 1H, ArH), 7.74 (d, *J* = 8.5Hz, 1H, ArH), 7.27 (m, 2H, ArH), 7.16 (s, 1H, ArH), 6.99 (d, *J* = 7.5Hz, 1H, ArH), 3.35 (dd, *J* = 9, 13.5Hz, 1H, CH₂), 3.09 (dd, *J* = 5.5, 13.5Hz, 1H, CH₂), 2.83 – 2.74 (m, 1H, CH), 1.40 (d, *J* = 7Hz, 3H, CH₃). ¹⁹F-NMR: (CDCl₃) δ -57.86, -62.34, ¹³C-NMR: (CDCl₃) δ 173.93 (C=O), 149.50 (ArC), 142.58 (ArC), 138.06 (ArC), 135.73 (ArCH), 133.91 (q, ²*J*_{C-F} = 32.4Hz, ArC), 130.21(ArCH), 127.10 (ArCH), 122.12 (q, ¹*J*_{C-F} = 272.5Hz, OCF₃), 121.93 (ArCH), 121.11 (ArCH), 120.33 (q, ¹*J*_{C-F} = 253.5Hz, CF₃), 118.53 (ArCH), 117.42 (q, ³*J*_{C-F} = 4.8Hz, ArCH), 115.89 (CN), 103.41 (ArC), 42.49 (CH), 36.72 (CH₂), 17.76 (CH₃). HRMS calcd for C₁₉H₁₄F₆N₂O₂S, 449.0753; found, 449.0752 [M+H], 466.1015 [M+NH₄⁺].

3-((4-Fluorophenyl)thio)-2-methyl-N-(4-nitro-3-(trifluoromethyl)phenyl)propanamide (18). Yield; 45 %

¹H NMR (CDCl₃) δ 8.36 (s, 1H, NH), 8.02 (d, *J* = 1.5 Hz, 1H, ArH), 7.98-7.95 (m, 2H, ArH), 7.38-7.33 (m, 2H, ArH), 6.99-6.94 (m, 2H, ArH), 3.27 (dd, *J* = 8.5, 13.5 Hz, 1H, CH₂), 3.03 (dd, *J* = 5, 13.5 Hz, 1H, CH₂), 2.72-2.64 (m, 1H, CH), 1.36 (d, *J* = 6.5 Hz, 3H, CH₃); ¹⁹F NMR (CDCl₃) δ -60.14, -114.70; ¹³C NMR (CDCl₃) δ 173.99 (C=O), 161.95 (d, ¹*J*_{C-F} = 245.8 Hz, ArC), 142.68 (ArC), 142.36 (ArC), 132.52 (d, ³*J*_{C-F} = 7.8 Hz, ArCH), 130.12 (d, ⁴*J*_{C-F} = 2.9 Hz, ArC), 127.12 (ArCH), 125.15 (q, ²*J*_{C-F} = 34.3 Hz, ArC), 122.23 (ArCH), 121.74 (q, ¹*J*_{C-F} = 271.9 Hz, CF₃), 118.16 (q, ³*J*_{C-F} = 6.1 Hz, ArCH), 116.23 (d, ²*J*_{C-F} = 21.9 Hz, ArCH), 42.56 (CH), 38.42 (CH₂), 17.72 (CH₃). MS [ESI, *m/z*]: HRMS calcd for C₁₇H₁₄F₄N₂O₃S [M+H], 403.0739; found, 403.0746.

2-Methyl-N-(4-nitro-3-(trifluoromethyl)phenyl)-3-((4-(trifluoromethyl)phenyl)thio)propanamide (19). Yield; 52 %

¹H NMR (CDCl₃) δ 8.00-7.92 (m, 3H, ArH), 7.74 (s, 1H, NH), 7.53 (d, *J* = 8 Hz, 2H, ArH), 7.41 (d, *J* = 8 Hz, 2H, ArH), 3.27 (dd, *J* = 9, 13.5 Hz, 1H, CH₂), 3.16 (dd, *J* = 5, 14 Hz, 1H, CH₂), 2.75-2.67 (m, 1H, CH), 1.44 (d, *J* = 7 Hz, 3H, CH₃); ¹⁹F NMR (CDCl₃) δ -60.13, -62.56; ¹³C NMR (CDCl₃) δ 173.16 (C=O), 143.13 (ArC), 141.71 (ArC), 140.58 (ArC), 128.25 (q, ²*J*_{C-F} = 32.6 Hz, ArC), 127.94 (ArCH), 127.10 (ArCH), 125.95 (q, ³*J*_{C-F} = 3.8 Hz, ArCH), 125.30 (q, ²*J*_{C-F} = 33.9 Hz, ArC), 122.13 (ArCH), 123.90 (q, ¹*J*_{C-F} = 270.3 Hz, CF₃), 121.66 (q, ¹*J*_{C-F} = 272.4 Hz, CF₃), 118.22 (q, ³*J*_{C-F} = 6 Hz, ArCH), 42.73 (CH), 35.92 (CH₂), 17.90 (CH₃). MS [ESI, *m/z*]: HRMS calcd for C₁₈H₁₄F₆N₂O₃S [M+H], 453.0702; found, 453.0699.

3-((3,5-Bis(trifluoromethyl)phenyl)thio)-N-(4-cyano-2-(trifluoromethyl)phenyl)-2-methylpropanamide (23). Yield; 41 %

^1H NMR (CDCl_3) δ 8.54 (d, J = 9 Hz, 1H, ArH), 7.92 (d, J = 1.5 Hz, 1H, ArH), 7.84 (dd, J = 2, 9 Hz, 1H, ArH), 7.75 (s, 1H, ArH), 7.70 (s, 1H, NH), 7.67 (s, 1H, ArH), 3.47 (dd, J = 8.5, 13.5 Hz, 1H, CH_2), 3.19 (dd, J = 5.5, 13.5 Hz, 1H, CH_2), 2.77-2.69 (m, 1H, CH), 1.45 (d, J = 7 Hz, 3H, CH_3); ^{19}F NMR (CDCl_3) δ -61.15, -63.10; ^{13}C NMR (CDCl_3) δ 172.43 (C=O), 139.27 (ArC), 138.79 (ArC), 136.69 (ArCH), 132.34 (q, $^2J_{\text{C-F}}$ = 33.3 Hz, ArC), 130.25 (q, $^3J_{\text{C-F}}$ = 5.4 Hz, ArCH), 128.38 (q, $^3J_{\text{C-F}}$ = 3.3 Hz, ArCH), 123.64 (ArCH), 122.89 (q, $^1J_{\text{C-F}}$ = 271.9 Hz, CF_3), 122.24 (ArC), 118.64 (q, $^1J_{\text{C-F}}$ = 304 Hz, CF_3), 120.01 (sept, $^3J_{\text{C-F}}$ = 3.8 Hz, ArCH), 117.43 (CN), 108.08 (ArC), 43.06 (CH), 36.62 (CH_2), 17.63 (CH_3). $\text{C}_{20}\text{H}_{13}\text{F}_9\text{N}_2\text{OS}$, MS (ES+) m/z : 523.0491 [$\text{M}+\text{Na}^+$], 518.0943 [$\text{M}+\text{NH}_4^+$].

3-((4-Fluorophenyl)thio)-2-methyl-N-(4-nitro-2-(trifluoromethyl)phenyl)propanamide (24). Yield; 49 %

^1H NMR (CDCl_3) δ 8.65 (d, J = 9 Hz, 1H, ArH), 8.52 (d, J = 2 Hz, 1H, ArH), 8.42 (dd, J = 2, 9 Hz, 1H, ArH), 7.84 (s, 1H, NH), 7.40 (dd, J = 5.5, 8.5 Hz, 2H, ArH), 7.01 (t, J = 8.5 Hz, 2H, ArH), 3.28 (dd, J = 8.5, 14 Hz, 1H, CH_2), 3.28 (dd, J = 5, 13.5 Hz, 1H, CH_2), 2.65 (sext, J = 7 Hz, 1H, CH), 1.38 (d, J = 7 Hz, 3H, CH_3); ^{19}F NMR (CDCl_3) δ -61.03, -114.95; ^{13}C NMR (CDCl_3) δ 173.15 (C=O), 162.14 (d, $^1J_{\text{C-F}}$ = 245.8 Hz, ArC), 142.89 (ArC), 140.76 (ArC), 133.03 (d, $^3J_{\text{C-F}}$ = 8 Hz, ArCH), 129.83 (d, $^4J_{\text{C-F}}$ = 3.4 Hz, ArC), 128.26 (ArCH), 123.36 (ArCH), 122.89 (q, $^1J_{\text{C-F}}$ = 272.1 Hz, CF_3), 122.32 (q, $^3J_{\text{C-F}}$ = 6 Hz, ArCH), 119.14 (q, $^2J_{\text{C-F}}$ = 31 Hz, ArC), 116.36 (d, $^2J_{\text{C-F}}$ = 22 Hz, ArCH), 43.05 (CH), 38.76 (CH_2), 17.41 (CH_3). MS [ESI, m/z]: HRMS calcd for $\text{C}_{17}\text{H}_{14}\text{F}_4\text{N}_2\text{O}_3\text{S}$ [$\text{M}+\text{H}$], 403.0734; found, 403.0733.

2-Methyl-N-(4-nitro-2-(trifluoromethyl)phenyl)-3-((4-(trifluoromethyl)phenyl)thio)propanamide (25). Yield; 56 %

^1H NMR (CDCl_3) δ 8.62 (d, J = 9 Hz, 1H, ArH), 8.52 (d, J = 2.5 Hz, 1H, ArH), 8.47 (dd, J = 2.5, 9 Hz, 1H, ArH), 7.81 (s, 1H, NH), 7.54 (d, J = 8 Hz, 2H, ArH), 7.43 (d, J = 8 Hz, 2H, ArH), 3.42 (dd, J = 8.5, 13.5 Hz, 1H, CH_2), 3.16 (dd, J = 5.5, 14 Hz, 1H, CH_2), 2.74 (sextet of triplet, J = 7, 1.5 Hz, 1H, CH), 1.44 (d, J = 7 Hz, 3H, CH_3); ^{19}F NMR (CDCl_3) δ -61.05, -62.58; ^{13}C NMR (CDCl_3) δ 172.84 (C=O), 140.58 (ArC), 140.49 (ArC), 128.36 (ArCH), 128.29 (q, $^2J_{\text{C-F}}$ = 32.5 Hz, ArC), 128.25 (ArCH), 125.91 (q, $^3J_{\text{C-F}}$ = 3.6 Hz, ArCH), 123.94 (q, $^1J_{\text{C-F}}$ = 270 Hz, CF_3), 122.85 (q, $^1J_{\text{C-F}}$ = 271.8 Hz, CF_3), 122.31 (q, $^3J_{\text{C-F}}$ = 5.6 Hz, ArCH), 119.25 (q, $^2J_{\text{C-F}}$ = 31.5 Hz, ArC), 43.03 (CH), 36.18 (CH_2), 17.51 (CH_3). MS [ESI, m/z]: HRMS calcd for $\text{C}_{18}\text{H}_{14}\text{F}_6\text{N}_2\text{O}_3\text{S}$ [$\text{M}+\text{H}$], 453.0708; found, 453.0711.

3-((3,5-Bis(trifluoromethyl)phenyl)thio)-2-methyl-N-(4-nitro-2-(trifluoromethyl)phenyl)**propanamide (26).** Yield; 24%

^1H NMR (CDCl_3) δ 8.64 (d, $J = 9.5$ Hz, 1H, ArH), 8.54 (d, $J = 3$ Hz, 1H, ArH), 8.43 (dd, $J = 2.5, 9.5$ Hz, 1H, ArH), 7.79 (s, 1H, NH), 7.76 (s, 2H, ArH), 7.01 (s, 1H, ArH), 3.48 (dd, $J = 8, 13.5$ Hz, 1H, CH_2), 3.21 (dd, $J = 5.5, 13.5$ Hz, 1H, CH_2), 2.76 (sextet of triplet, $J = 7, 1.5$ Hz, 1H, CH), 1.47 (d, $J = 7$ Hz, 3H, CH_3); ^{19}F NMR (CDCl_3) δ -61.10, -63.11; ^{13}C NMR (CDCl_3) δ 172.47 (C=O), 143.09 (ArC), 140.41 (ArC), 139.21 (ArC), 132.38 (q, $^2J_{\text{C-F}} = 33.3$ Hz, ArC), 128.40 (d, $^4J_{\text{C-F}} = 3.3$ Hz, ArCH), 128.31 (ArCH), 123.30 (ArCH), 122.87 (q, $^1J_{\text{C-F}} = 271.1$ Hz, CF_3), 122.85 (q, $^1J_{\text{C-F}} = 271.9$ Hz, CF_3), 122.34 (q, $^3J_{\text{C-F}} = 5.9$ Hz, ArCH), 119.30 (q, $^2J_{\text{C-F}} = 31.1$ Hz, ArC), 120.06 (sept, $^3J_{\text{C-F}} = 3.6$ Hz, ArCH), 43.13 (CH), 36.62 (CH_2), 17.63 (CH_3). MS [ESI, m/z]: HRMS calcd for $\text{C}_{19}\text{H}_{13}\text{F}_9\text{N}_2\text{O}_3\text{S}$ [M+H], 521.0573; found, 521.0576.

N-(4-cyano-3-(trifluoromethyl)phenyl)-2-methyl-2,3-bis((4-(trifluoromethyl)phenyl)thio)**propanamide (27).** Yield; 42%

^1H -NMR: (CDCl_3) δ 9.06 (s, 1H, NH), 7.97 (d, $J = 2$ Hz, 1H ArH), 7.85 (dd, $J = 2, 8.5$ Hz, 1H, Ar-H), 7.79 (d, $J = 8.5$ Hz, 1H, ArH), 7.59 (d, $J = 8.5$ Hz, 2H, ArH), 7.51 (d, $J = 8$ Hz, 2H, ArH), 7.44 (dd, $J = 8.5, 13.5$ Hz, 4H, ArH), 3.60 (d, $J = 13.5$ Hz, 1H, CH_2), 3.52 (d, $J = 13.5$ Hz, 1H, CH_2), 1.73 (s, 3H, CH_3). ^{19}F -NMR: (CDCl_3) δ -62.23, -62.65, -63.00. ^{13}C -NMR: (CDCl_3) δ 170.74 (C=O), 141.22 (ArC), 140.60 (ArC), 135.86 (ArCH), 134.35 (ArCH), 134.23 (ArC), 134.11 (q, $^2J_{\text{C-F}} = 31$ Hz, ArC), 131.69 (q, $^2J_{\text{C-F}} = 33.1$ Hz, ArC), 131.26 (ArCH), 129.00 (ArCH), 128.64 (q, $^2J_{\text{C-F}} = 32.6$ Hz, ArC), 126.35 (q, $^3J_{\text{C-F}} = 3.6$ Hz, ArCH), 125.89 – 125.74 (m, ArCH), 123.77 (q, $^1J_{\text{C-F}} = 270$ Hz, CF_3), 123.51 (q, $^1J_{\text{C-F}} = 270.8$ Hz, CF_3), 122.00 (q, $^1J_{\text{C-F}} = 272.3$ Hz, CF_3), 117.14 (q, $^3J_{\text{C-F}} = 5$ Hz, ArCH), 115.30 (CN), 105.04 (ArC), 59.51 (-C- CH_3), 42.06 (CH_2), 23.87 (CH_3). HRMS calcd for $\text{C}_{26}\text{H}_{17}\text{F}_9\text{N}_2\text{OS}_2$, 609.0711; found, 609.0708 [M+H], 626.0965 [M+ NH_4^+].

2,3-Bis((3,5-bis(trifluoromethyl)phenyl)thio)-2-methyl-N-(4-nitro-2-(trifluoromethyl)phenyl)**propanamide (28).** Yield; 48 %

^1H NMR (CDCl_3) δ 9.19 (s, 1H, NH), 8.59 (d, $J = 3$ Hz, 1H, ArH), 8.54 (d, $J = 9.5$ Hz, 1H, ArH), 8.45 (dd, $J = 2.5, 9$ Hz, 1H, ArH), 7.92 (s, 1H, ArH), 7.89 (s, 2H, ArH), 7.78 (s, 2H, ArH), 7.67 (s, 1H, ArH), 3.63 (d, $J = 13.5$ Hz, 1H, CH_2), 3.49 (d, $J = 13.5$ Hz, 1H, CH_2), 1.80 (s, 3H, CH_3); ^{19}F NMR (CDCl_3) δ -61.05, -63.14, 63.19; ^{13}C NMR (CDCl_3) δ 169.75 (C=O), 143.34 (ArC), 139.89 (ArC), 138.78 (ArC), 132.30 (ArC), 132.87 (q, $^2J_{\text{C-F}} = 33.9$ Hz, ArC), 132.42 (q, $^2J_{\text{C-F}} = 33.3$ Hz, ArC), 134.69, 134.66 (ArCH), 129.58 (d, $^3J_{\text{C-F}} = 3.6$ Hz, ArCH), 128.53 (ArCH), 122.44 (q, $^1J_{\text{C-F}} = 271.6$ Hz, CF_3), 123.87 (septet, $^3J_{\text{C-F}} = 3.6$ Hz, ArCH), 122.53 (q, $^3J_{\text{C-F}} = 5.5$ Hz, ArCH), 122.88 (q, $^1J_{\text{C-F}} = 272.3$ Hz, CF_3), 122.75 (q, $^1J_{\text{C-F}} = 274.4$ Hz, CF_3), 122.31 (ArCH),

120.72 (septet, $^3J_{\text{C-F}} = 3.9$ Hz, ArCH), 119.29 (q, $^2J_{\text{C-F}} = 31.5$ Hz, ArC), 57.94 (CH₃C), 42.43 (CH₂), 14.15 (CH₃). MS [ESI, m/z]: HRMS for C₂₇H₁₅F₁₅N₂O₃S₂ [M+H], 765.0371.

4.1.3 General method for the preparation of sulfones derivatives 29-41

To a stirring solution of the corresponding sulfide **14-26** (0.7 mmol) in 5 mL anhydrous dichloromethane, was added 3-chloroperbenzoic acid (MCPBA) (1.4 mmol). The solution was stirred at room temperature for 24 h. The reaction mixture was neutralized with 1M sodium hydroxide. 50 mL distilled water was added to the reaction mixture and was extracted with 2 x 50mL of dichloromethane. The combined organic layers were washed, dried over anhydrous sodium sulfate, and concentrated *in vacuo*. The crude residue was purified by column chromatography, preparative TLC or crystallization from methanol.

N-(4-cyano-3-(trifluoromethyl)phenyl)-3-((4-fluorophenyl)sulfonyl)-2-methylpropanamide (29).

Yield; 69%

$^1\text{H-NMR}$: ((CD₃)₂SO) δ 10.82 (s, 1H, NH), 8.12 (d, $J = 2$ Hz, 1H, ArH), 8.09 (d, $J = 8.5$ Hz, 1H, ArH), 7.94 (dd, $J = 5, 9$ Hz, 2H, ArH), 7.82 (dd, $J = 2, 8$ Hz, 1H, ArH), 7.38 (t, $J = 9$ Hz, 2H, ArH), 3.81 (dd, $J = 9.5, 14.5$ Hz, 1H, CH₂), 3.50 (dd, $J = 4, 14.5$ Hz, 1H, CH₂), 3.06 – 2.98 (m, 1H, CH), 1.23 (d, $J = 7.5$ Hz, 3H, CH₃).

$^{19}\text{F-NMR}$: ((CD₃)₂SO) δ -61.34, -104.87, $^{13}\text{C NMR}$ ((CD₃)₂SO) δ 173.24 (C=O), 165.56 (d, $^1J_{\text{C-F}} = 250$ Hz, ArC), 143.76 (ArC), 136.92 (ArCH), 135.71 (ArC), 132.13 (q, $^2J_{\text{C-F}} = 31.5$ Hz, ArC), 131.61 (d, $^3J_{\text{C-F}} = 9.9$ Hz, ArCH), 122.86 (q, $^1J_{\text{C-F}} = 273.3$ Hz, CF₃), 122.49 (ArCH), 116.93 (d, $^2J_{\text{C-F}} = 22.6$ Hz, ArCH), 116.84 (m, ArCH), 116.21 (CN), 102.26 (ArC), 57.72 (CH₂), 36.81 (CH), 18.76 (CH₃). HRMS calcd for C₁₈H₁₄F₄N₂O₃S [M+H], 415.0734; found, 415.0735, [M+NH₄⁺], 432.0999.

N-(4-cyano-3-(trifluoromethyl)phenyl)-2-methyl-3-((4-(trifluoromethyl)phenyl)sulfonyl)propanamide (30). Yield; 21%

$^1\text{H-NMR}$: (CDCl₃) δ 8.88 (s, 1H, NH), 8.12 (d, $J = 8.5$ Hz, 2H ArH), 7.96 (d, $J = 2$ Hz, 1H, ArH), 7.88 – 7.83 (m, 3H, ArH), 7.72 (d, $J = 8.5$ Hz, 1H, ArH), 3.99 (dd, $J = 9.5, 14$ Hz, 1H, CH₂), 3.43 – 3.35 (m, 1H, CH), 3.22 (dd, $J = 3, 14$ Hz, 1H, CH₂), 1.43 (d, $J = 7.5$ Hz, 3H, CH₃). $^{19}\text{F-NMR}$: (CDCl₃) δ -62.31, -63.42. $^{13}\text{C-NMR}$: (CDCl₃) δ 172.27 (C=O), 142.37 (ArC), 142.25 (ArC), 136.04 (q, $^2J_{\text{C-F}} = 33$ Hz, ArC), 135.75 (ArCH), 133.72 (q, $^2J_{\text{C-F}} = 32.5$ Hz, ArC), 128.65 (ArCH), 126.67 (q, $^3J_{\text{C-F}} = 3.6$ Hz, ArCH), 122.87 (q, $^1J_{\text{C-F}} = 271.6$ Hz, CF₃), 122.07 (q, $^1J_{\text{C-F}} = 272.5$ Hz, CF₃), 121.81 (ArCH), 117.18 (q, $^3J_{\text{C-F}} = 4.9$ Hz, ArCH), 115.52 (CN), 104.40 (ArC), 58.88 (-CH₂), 36.69 (CH), 18.88 (CH₃). HRMS calculated for C₁₉H₁₄F₆N₂O₃S [M+H], 465.0708; found, 465.0703.

3-((3,5-Bis(trifluoromethyl)phenyl)sulfonyl)-N-(4-cyano-3-(trifluoromethyl)phenyl)-2-methylpropanamide (31). Yield; 19%

¹H-NMR: (CDCl₃) δ 8.38 (s, 1H, NH), 8.30 (s, 2H, ArH), 8.06 (s, 1H, ArH), 7.88 (d, J = 2Hz, 1H, ArH), 7.74 (dd, J = 2, 8.5Hz, 1H, ArH), 7.68 (d, J = 8.5Hz, 1H, ArH), 3.91 (dd, J = 9.5, 14.5Hz, 1H, CH₂), 3.29 – 3.21 (m, 1H, CH), 3.17 (dd, J = 3.5, 14.5Hz, 1H, CH₂), 1.37 (d, J = 7Hz, 3H, CH₃). ¹⁹F-NMR: (CDCl₃) δ -62.38, -63.04. ¹³C-NMR: (CDCl₃) δ 171.78 (C=O), 141.89 (ArC), 141.81 (ArC), 135.82 (ArCH), 134.03 (q, ²J_{C-F} = 32.6Hz, ArC), 133.43 (q, ²J_{C-F} = 34.6Hz, ArC), 128.43 (q, ³J_{C-F} = 3Hz, ArCH), 128.01 – 127.77 (m, ArCH), 122.14 (q, ¹J_{C-F} = 271.8Hz, CF₃), 122.00 (q, ¹J_{C-F} = 272.4Hz, CF₃), 121.79 (ArCH), 117.23 (q, ³J_{C-F} = 4.6Hz, ArCH), 115.52 (CN), 104.40 (ArC), 58.88 (CH₂), 36.69 (CH), 18.88 (CH₃). HRMS calculated for C₂₀H₁₃F₉N₂O₃S [M+H], 533.0576; found, 533.0572.

***N*-(4-cyano-3-(trifluoromethyl)phenyl)-2-methyl-3-((3-(trifluoromethoxy)phenyl)sulfonyl)propanamide (32).** Yield; 95%

¹H-NMR: (CDCl₃) δ 8.67 (s, 1H, NH), 7.88 (d, J = 2Hz, 1H, ArH), 7.82 (d, J = 7.5Hz, 1H, ArH), 7.77 (dd, J = 2, 8.5Hz, 1H, ArH), 7.72 (s, 1H, ArH), 7.63 (d, J = 8.5Hz, 1H, ArH), 7.57 (t, J = 8Hz, 1H, ArH), 7.45 (d, J = 8.5Hz, 1H, ArH), 3.86 (dd, J = 9.5, 14Hz, 1H, CH₂), 3.34 – 3.25 (m, 1H, CH), 3.12 (dd, J = 3.5, 14.5Hz, 1H, CH₂), 1.34 (d, J = 7Hz, 3H, CH₃). ¹⁹F-NMR: (CDCl₃) δ -58.04, -62.34. ¹³C-NMR: (CDCl₃) δ 171.69 (C=O), 149.10 (ArC), 141.72 (ArC), 140.37 (ArC), 135.21 (ArCH), 133.28 (q, ²J_{C-F} = 32.8Hz, ArC), 130.95 (ArCH), 126.19 (ArCH), 125.65 (ArCH), 121.55 (q, ¹J_{C-F} = 272.3Hz, OCF₃), 121.30 (ArCH), 119.92 (ArCH), 119.68 (q, ¹J_{C-F} = 258.3Hz, CF₃), 116.76 (q, ³J_{C-F} = 4.8Hz, ArCH), 115.05 (CN), 103.58 (ArC), 58.43 (CH₂), 35.82 (-CH), 18.46 (CH₃). HRMS calculated for C₁₉H₁₄F₆N₂O₄S [M+H], 481.0657; found, 481.0654.

3-((4-Fluorophenyl)sulfonyl)-2-methyl-*N*-(4-nitro-3-(trifluoromethyl)phenyl)propanamide (33).

Yield; 41 %

¹H NMR (CD₃OD) δ 8.14 (d, J = 2 Hz, 1H, ArH), 8.14 (d, J = 2 Hz, 1H, ArH), 8.01-7.97 (m, 2H, ArH), 7.88 (dd, J = 2, 9 Hz, 1H, ArH), 7.32-7.26 (m, 2H, ArH), 3.91 (dd, J = 9.5, 14.5 Hz, 1H, CH₂), 3.34 (dd, J = 3, 14.5 Hz, 1H, CH₂), 3.17-3.08 (m, 1H, CH), 1.34 (d, J = 7.5 Hz, 3H, CH₃); ¹⁹F NMR (CD₃OD) δ -61.67, -105.84; ¹³C NMR (CD₃OD) δ 175.65 (C=O), 168.31 (d, ¹J_{C-F} = 253.5 Hz, ArC), 145.40 (ArC), 145.01 (ArC), 137.66 (d, ⁴J_{C-F} = 3.3 Hz, ArC), 133.52 (d, ³J_{C-F} = 9.9 Hz, ArCH), 129.05 (ArCH), 126.38 (q, ²J_{C-F} = 33.5 Hz, ArC), 124.53 (ArCH), 124.46 (q, ¹J_{C-F} = 270.9 Hz, CF₃), 119.95 (q, ³J_{C-F} = 5.8 Hz, ArCH), 118.53 (d, ²J_{C-F} = 23.3 Hz, ArCH), 60.25 (CH₂), 39.09 (CH), 20.14 (CH₃). MS [ESI, m/z]: HRMS calcd for C₁₇H₁₄F₄N₂O₅S [M+H], 435.0638; found, 435.0643.

2-Methyl-*N*-(4-nitro-3-(trifluoromethyl)phenyl)-3-((4-(trifluoromethyl)phenyl)sulfonyl)propanamide (34).

Yield; 78 %

¹H NMR (CDCl₃) δ 8.77 (s, 1H, NH), 8.15-8.11 (m, 3H, ArH), 7.96 (dd, J = 9, 2.5 Hz, 1H, ArH), 7.94-7.91 (m, 1H, ArH), 7.90-7.87 (m, 2H, ArH), 3.97 (dd, J = 9.5, 14 Hz, 1H, CH₂), 3.45-3.35 (m, 1H, CH), 3.22

(dd, $J = 3, 14$ Hz, 1H, CH_2), 1.45 (d, $J = 7$ Hz, 3H, CH_3); ^{19}F NMR (CDCl_3) δ -60.18, -63.35; ^{13}C NMR (CDCl_3) δ 172.02 (C=O), 143.06 (ArC), 142.22 (ArC), 141.96 (ArC), 136.20 (q, $^2J_{\text{C-F}} = 33.3$ Hz, ArC), 128.58 (ArCH), 127.02 (ArCH), 126.79 (q, $^3J_{\text{C-F}} = 3.6$ Hz, ArCH), 125.15 (q, $^2J_{\text{C-F}} = 33.8$ Hz, ArC), 122.87 (q, $^1J_{\text{C-F}} = 271.4$ Hz, CF_3), 122.12 (ArCH), 121.65 (q, $^1J_{\text{C-F}} = 271.9$ Hz, CF_3), 118.22 (q, $^3J_{\text{C-F}} = 5.6$ Hz, ArCH), 58.98 (CH_2), 36.22 (CH), 18.94 (CH_3). MS [ESI, m/z]: HRMS calcd for $\text{C}_{18}\text{H}_{14}\text{F}_6\text{N}_2\text{O}_5\text{S}$ [$\text{M}+\text{NH}_4$], 502.0866; found, 502.0857.

3-((3,5-Bis(trifluoromethyl)phenyl)sulfonyl)-2-methyl-*N*-(4-nitro-3-(trifluoromethyl) phenyl) propanamide (35). Yield; 69%

^1H NMR (CD_3OD) δ 8.48 (s, 2H, ArH), 8.25 (s, 1H, ArH), 8.04 (d, $J = 1.5$ Hz, ArH), 8.01 (d, $J = 9$ Hz, 1H, ArH), 7.78 (dd, $J = 1.5, 9$ Hz, 1H, ArH), 4.13 (dd, $J = 10.5, 15$ Hz, 1H, CH_2), 3.51 (dd, $J = 3, 15$ Hz, 1H, CH_2), 3.23-3.15 (m, 1H, CH), 1.36 (d, $J = 7$ Hz, 3H, CH_3); ^{19}F NMR (CD_3OD) δ -61.79, -64.50; ^{13}C NMR (CD_3OD) δ 172.90 (C=O), 142.79 (ArC), 142.71 (ArC), 142.01 (ArC), 132.65 (q, $^2J_{\text{C-F}} = 38.8$ Hz, ArC), 128.44 (q, $^3J_{\text{C-F}} = 3$ Hz, ArCH), 127.44 (q, $^3J_{\text{C-F}} = 3$ Hz, ArCH), 126.67 (ArCH), 125.58 (m, ArC), 124.31 (m, ArC), 123.33 (q, $^1J_{\text{C-F}} = 270.3$ Hz, CF_3), 122.01 (ArCH), 121.9 (q, $^1J_{\text{C-F}} = 270.9$ Hz, CF_3), 117.68 (m, ArCH), 57.70 (CH_2), 36.74 (CH), 18.23 (CH_3). MS [ESI, m/z]: HRMS calcd for $\text{C}_{19}\text{H}_{13}\text{F}_9\text{N}_2\text{O}_5\text{S}$ [$\text{M}+\text{NH}_4$], 570.0740; found, 570.0733.

***N*-(4-cyano-2-(trifluoromethyl)phenyl)-3-((4-fluorophenyl)sulfonyl)-2-methylpropanamide (36).**

Yield; 68 %

^1H NMR (CDCl_3) δ 8.41 (d, $J = 8.5$ Hz, 1H, ArH), 8.00-7.95 (m, 3H, ArH), 7.86 (dd, $J = 1.5, 8.5$ Hz, 1H, ArH), 7.83 (s, 1H, NH), 7.28-7.24 (m, 2H, ArH), 3.85-3.79 (m, 1H, CH_2), 3.21-3.14 (m, 2H, CH, CH_2), 1.45 (d, $J = 7$ Hz, 3H, CH_3); ^{19}F NMR (CDCl_3) δ -61.04, -102.36; ^{13}C NMR (CDCl_3) δ 171.66 (C=O), 166.08 (d, $^1J_{\text{C-F}} = 256.3$ Hz, ArC), 138.82 (ArC), 136.59 (ArCH), 135.19 (ArC), 135.16 (ArC), 130.89 (d, $^3J_{\text{C-F}} = 9.4$ Hz, ArCH), 130.28 (q, $^3J_{\text{C-F}} = 5.5$ Hz, ArCH), 124.51 (ArCH), 122.84 (q, $^1J_{\text{C-F}} = 271.6$ Hz, CF_3), 117.25 (CN), 116.88 (d, $^2J_{\text{C-F}} = 22.6$ Hz, ArCH), 108.42 (ArC), 58.99 (CH_2), 37.06 (CH), 18.50 (CH_3). MS [ESI, m/z]: HRMS calcd for $\text{C}_{18}\text{H}_{14}\text{F}_4\text{N}_2\text{O}_3\text{S}$ [$\text{M}+\text{H}$], 415.0734; found, 415.0733.

***N*-(4-cyano-2-(trifluoromethyl)phenyl)-2-methyl-3-((4-(trifluoromethyl)phenyl)sulfonyl) propanamide (37).** Yield; 71 %

^1H NMR (CD_3OD) δ 8.20 (d, $J = 8$ Hz, 2H, ArH), 8.16 (d, $J = 2$ Hz, 1H, ArH), 8.02-7.99 (m, 3H, ArH), 7.76 (d, $J = 8.5$ Hz, 1H, ArH), 3.92 (dd, $J = 9.5, 14$ Hz, 1H, CH_2), 3.43 (dd, $J = 3.5, 14.5$ Hz, 1H, CH_2), 3.32-3.25 (m, 1H, CH), 1.34 (d, $J = 7$ Hz, 3H, CH_3); ^{19}F NMR (CD_3OD) δ -62.52, -64.66; ^{13}C NMR (CD_3OD) δ 173.92 (C=O), 143.13 (ArC), 139.04 (q, $^3J_{\text{C-F}} = 1.5$ Hz, ArC), 136.03 (ArCH), 134.96 (q, $^2J_{\text{C-F}} = 32.9$ Hz, ArC),

130.44 (q, $^3J_{C-F}$ = 5.4 Hz, ArCH), 129.84 (ArCH), 128.85 (ArCH), 126.31 (q, $^3J_{C-F}$ = 3.8 Hz, ArCH), 125.35 (q, $^2J_{C-F}$ = 30.8 Hz, ArC), 123.39 (q, $^1J_{C-F}$ = 270.9 Hz, CF₃), 122.61 (q, $^1J_{C-F}$ = 271.6 Hz, CF₃), 116.82 (CN), 110.13 (ArC), 57.47 (CH₂), 35.43 (CH), 17.56 (CH₃). MS [ESI, m/z]: HRMS calcd for C₁₉H₁₄F₆N₂O₃S [M+H], 465.0702; found, 465.0699.

3-((3,5-Bis(trifluoromethyl)phenyl)sulfonyl)-N-(4-cyano-2-(trifluoromethyl)phenyl)-2-methylpropanamide (38). Yield; 59 %

1H NMR (CDCl₃) δ 8.40 (s, 1H, ArH), 8.38 (d, J = 9 Hz, 1H, ArH), 8.18 (s, 1H, ArH), 7.96 (s, 1H, ArH), 7.86 (d, J = 9 Hz, 1H, ArH), 7.81 (s, 1H, NH), 3.47 (dd, J = 10, 15 Hz, 1H, CH₂), 3.31-3.23 (m, 2H, CH₂, CH), 1.50 (d, J = 7 Hz, 3H, CH₃); ^{19}F NMR (CDCl₃) δ -61.04, -62.95; ^{13}C NMR (CDCl₃) δ 171.21 (C=O), 142.14 (ArC), 138.55 (ArC), 136.65 (ArCH), 133.40 (q, $^2J_{C-F}$ = 35 Hz, ArC), 132.32 (q, $^3J_{C-F}$ = 5.5 Hz, ArCH), 128.44 (q, $^3J_{C-F}$ = 3.4 Hz, ArCH), 127.81 (sept, $^3J_{C-F}$ = 3.8 Hz, ArCH), 124.27 (ArCH), 122.84 (q, $^1J_{C-F}$ = 271.8 Hz, CF₃), 122.66 (ArC), 117.56 (q, $^1J_{C-F}$ = 281.5 Hz, CF₃), , 117.16 (CN), 108.64 (ArC), 58.77 (CH₂), 37.12 (CH), 18.56 (CH₃). MS (ES+) m/z: C₂₀H₁₃F₉N₂O₃S, 550.084 [M+NH₄⁺], 555.0395 [M+Na⁺].

3-((4-Fluorophenyl)sulfonyl)-2-methyl-N-(4-nitro-2-(trifluoromethyl)phenyl)propanamide (39).

Yield; 72 %

1H NMR (CDCl₃) δ 8.53 (d, J = 2 Hz, 1H, ArH), 8.44-8.39 (m, 2H, ArH), 8.04 (s, 1H, NH), 7.97 (dd, J = 5, 9 Hz, 2H, ArH), 7.25 (t, J = 8.5 Hz, 2H, ArH), 3.84 (dd, J = 8.5, 14 Hz, 1H, CH₂), 3.30-3.22 (m, 1H, CH), 3.17 (dd, J = 4, 14 Hz, 1H, CH₂), 1.44 (d, J = 7.5 Hz, 3H, CH₃); ^{19}F NMR (CDCl₃) δ -60.99, -102.41; ^{13}C NMR (CDCl₃) δ 170.91 (C=O), 165.02 (d, $^1J_{C-F}$ = 255 Hz, ArC), 143.40 (ArC), 140.49 (ArC), 135.13 (d, $^4J_{C-F}$ = 3 Hz, ArC), 130.89 (d, $^3J_{C-F}$ = 9.9 Hz, ArCH), 128.05 (ArCH), 124.67 (ArCH), 122.73 (q, $^1J_{C-F}$ = 271.9 Hz, CF₃), 122.33 (q, $^3J_{C-F}$ = 5.8 Hz, ArCH), 120.50 (q, $^2J_{C-F}$ = 31.1 Hz, ArC), 116.86 (d, $^2J_{C-F}$ = 22.6 Hz, ArCH), 58.21 (CH₂), 36.88 (CH), 18.53 (CH₃). HRMS calcd for C₁₇H₁₄F₄N₂O₅S [M+H], 435.0632; found, 435.0631.

2-Methyl-N-(4-nitro-2-(trifluoromethyl)phenyl)-3-((4-(trifluoromethyl)phenyl)sulfonyl)propanamide (40). Yield; 74 %

1H NMR (CDCl₃) δ 8.56 (d, J = 2 Hz, 1H, ArH), 8.48-8.40 (m, 2H, ArH), 8.10 (d, J = 8.5 Hz, 2H, ArH), 7.91 - 7.84 (m, 2H, ArH, 1H, NH), 3.89 (dd, J = 9.5, 15 Hz, 1H, CH₂), 3.26-3.16 (m, 1H, CH₂, 1H, CH), 1.48 (d, J = 7 Hz, 3H, CH₃); ^{19}F NMR (CDCl₃) δ -60.93, 60.97, -63.28; ^{13}C NMR (CDCl₃) δ 171.51 (C=O), 143.41 (ArC), 142.58 (ArC), 140.32 (ArC), 135.88 (q, $^2J_{C-F}$ = 32.9 Hz, ArC), 128.70 (ArCH), 128.19 (ArCH), 126.64 (q, $^3J_{C-F}$ = 3.6 Hz, ArCH), 124.15 (ArCH), 122.95 (q, $^1J_{C-F}$ = 271.8 Hz, CF₃), 122.79 (q, $^1J_{C-F}$ = 271.9 Hz, CF₃),

122.36 (q, $^3J_{C-F}$ = 5.5 Hz, ArCH), 120.12 (q, $^2J_{C-F}$ = 30.9 Hz, ArC), 58.67 (CH), 37.08 (CH₂), 18.57 (CH₃). MS [ESI, m/z]: HRMS calcd for C₁₈H₁₄F₆N₂O₅S [M+H], 485.0600; found, 485.0595.

3-((3,5-Bis(trifluoromethyl)phenyl)sulfonyl)-2-methyl-N-(4-nitro-2-(trifluoromethyl)phenyl)

propanamide (41). Yield; 58 %.

1H NMR ((CD₃)₂SO) δ 10.10 (s, 1H, NH), 8.65 (s, 1H, ArH), 8.55 (s, 2H, ArH), 8.52 (d, J = 8.5 Hz, 1H, ArH), 8.46 (d, J = 2 Hz, 1H, ArH), 7.72 (d, J = 8.5 Hz, 1H, ArH), 4.01 (dd, J = 9, 14.5 Hz, 1H, CH₂), 3.84 (dd, J = 3, 14 Hz, 1H, CH₂), 3.34 (m, 1H, CH), 1.26 (d, J = 7 Hz, 3H, CH₃); ^{19}F NMR ((CD₃)₂SO) δ -59.84, -61.32; ^{13}C NMR ((CD₃)₂SO) δ 173.28 (C=O), 144.86 (ArC), 142.40 (ArC), 141.27 (ArC), 131.92 (q, $^2J_{C-F}$ = 34 Hz, ArC), 130.21 (ArCH), 129.29 (d, $^4J_{C-F}$ = 3.4 Hz, ArCH), 128.65 (m, ArCH), 128.33 (ArCH), 124.06 (q, $^2J_{C-F}$ = 31.4 Hz, ArC), 122.79 (q, $^1J_{C-F}$ = 275.3 Hz, CF₃), 123.01 (q, $^1J_{C-F}$ = 271.8 Hz, CF₃), 122.68 (q, $^3J_{C-F}$ = 5.5 Hz, ArCH), 56.86 (CH₂), 35.22 (CH), 18.70 (CH₃). MS [ESI, m/z]: HRMS calcd for C₁₉H₁₃F₉N₂O₅S [M+NH₄], 570.0740; found, 570.0736.

4.2 In vitro cell based assay

4.2.1 Cell culture

All cells were cultured in T75 flasks in a humidified atmosphere of 5% CO₂ at 37°C. LNCaP cells were cultured in RPMI-1640 medium, PC3 and VCaP cells in DMEM, all supplemented with 10% FCS and antibiotics (penicillin 100U/ml and streptomycin 100µg).

4.2.2 Anti-androgen treatment in vitro

Bicalutamide and enzalutamide were used as positive controls (used as the clinical standard) in LNCaP, PC3 and VCaP cells, and DMSO was used as a vehicle control. Nine 1/2 serial dilutions of 10 mM bicalutamide stock were made in 50 µL of DMSO to give nine increasing concentrations from 0.1 µM to 100 µM. All novel deshydroxy compounds were tested in LNCaP cells, and compounds **27**, **28** and **33** were subsequently tested in PC3 and VCaP cells because of their low IC₅₀ values.

PC3 and LNCaP cells were plated in a 96- well plate (4000cells/well) and then incubated overnight to adhere. Each drug concentration (0-100uM) was then added in sequence to ten tubes of fresh media to achieve a 1:100 dilution. The old medium was then gently removed and replaced with 200 µL of fresh media containing the nine increasing drug concentrations and the DMSO control, in triplicate. Following 96 hours of incubation the samples were tested with the MTT or MTS assay. The IC₅₀ was then calculated from the mean of these triplicate values and dose-response curves were plotted. VCaP cells were treated as above, with the following exceptions. The novel compounds were diluted 1:50, only 100 µL of the old medium was extracted and it was replaced with 100 µL of the novel

compound in media. This was done to avoid removing the cells from the 96-well plates in view of their poor adherence.

4.2.3 MTT and MTS assays

Colorimetric MTT (LNCaP and PC3) and MTS (VCaP) assays were used to determine cell viability following *in vitro* anti-androgen treatment. 20 μ L (1/10th well volume) of MTT or MTS were added to the wells as appropriate. MTS absorbance was recorded at 490 nm by the Elx800TM microplate reader after 1 and 2-hours of incubation. For the MTT assay, following the appearance of purple formazan crystals under the light microscope, the medium was then carefully removed and the formazan crystals dissolved in 200 μ L of acidified isopropanol and MTT absorbance was recorded at 540nm on the Elx800TM microplate reader. Percentage cell viability was normalised to the DMSO control.

4.2.4 Statistics

Cell number-MTT correlations and IC₅₀ values were calculated from the mean of three replicates using Microsoft Excel and GraphPad Prism v6.01 (GraphPad Software, Inc., San Diego, CA). Cell number-MTT correlations were analysed by linear regression, whereas IC₅₀ values were produced through non-linear regression. qPCR results were analysed using the $\Delta\Delta$ CT method in Excel. Mean IC₅₀ values were then analysed for statistical significance ($p < 0.05$) compared to bicalutamide and enzalutamide using GraphPad Prism v6.01 with consideration to the OECD guidelines.

One-way analysis of variance (ANOVA) followed by Tukey's Honest Significant Difference test analysed the dose-response data for compounds **27**, **28** and **33** in LNCaP cells, which satisfied the assumptions of normality and homogeneity of variance according to the D'Agostino- Pearson omnibus, Brown-Forsythe and Bartlett's tests. The Kruskal-Wallis test followed by the Dunn's test analysed the dose-response data for compound **28** in LNCaP cells and compounds **27**, **28** and **33** in PC3 cells.

4.3 PSA Expression and androgen inhibition qPCR experiments

LNCaP cells were trypsinised and re-suspended in 13ml of RPMI. 0.5ml of this cell suspension was then added to individual wells in 6-well plates with 3 ml of fresh RPMI, and the cells incubated for 24-hours to adhere. Two individual wells in each plate received no treatment and DMSO at a 1:100 dilution as negative controls. The 6-well plates used to analyse PSA expression by qPCR then were treated with 5, 10, 50 and 100 μ M of bicalutamide, compounds **27**, **28** and **33**, followed by 24-hours incubation.

4.3.1 RNA Isolation

RNA isolation was carried out in the six-well plates using the Sigma procedure. The media was gently removed, 1ml of TRI-reagent added per sample and the viscous lysate containing DNA, RNA and proteins transferred to 1.5ml Eppendorf tubes. 200 μ l of 1-bromo-3-chloropropane was then added, the Eppendorf tubes vortexed, left to stand for 5 minutes and stored at -80°C. The samples were then warmed to room temperature, vortexed and centrifuged at 12,000 x g for 15 minutes at 4°C to solubilise the RNA in the upper, colourless aqueous phase. The samples were then kept on ice, the aqueous phase transferred to fresh Eppendorf tubes and 0.5ml of isopropanol added. The tubes were then vortexed, left to stand for 5 minutes and centrifuged at 12,000 x g for 10 minutes at 4°C in order to recover the RNA pellet. After removing the supernatant, the pellet was washed with 1ml of 75% ethanol, vortexed and centrifuged at 7500 x g for 5 minutes at 4°C. After this, ethanol was carefully removed, the samples briefly air-dried for 5-10 minutes and the RNA pellet dissolved with 20 μ l of RNase-free PCR water. The RNA concentration was then measured in ng/ μ l by recording the absorption of each 1 μ l sample at 260nm on the Implen NanoPhotometer against nuclease-free water as a control. The samples were then stored at -80°C for 24 hours.

4.3.2 Complementary DNA synthesis (cDNA)

The RNA samples were uniformly diluted to 50ng/ μ l on ice. 10 μ l of RNA and 10 μ l of RT mix were then centrally added to a 96-well non-skirted PCR plate on ice, thermosealed and centrifuged up to 1000rpm in the Grant bio LMC-3000. The components of the RT mix are shown below: The samples were then placed in the Simpli-Amp thermal cycler under the following conditions: 25°C for 5 minutes, 42°C for 60 minutes, 70°C for 15 minutes, and 4°C. The samples were then stored at -20°C overnight.

4.3.3 Quantitative polymerase chain reaction (qPCR)

qPCR was performed in triplicate to analyse the LNCaP cells for relative PSA gene expression. The PSA primer was run alongside the AR, GAPDH, RPL19 and B-actin as housekeeping genes in order to normalise the data and validate the results. These forward and reverse primer pairs were briefly thawed and vortexed, diluted 1:40 with RNase-free PCR water in four 1.5ml Eppendorf tubes, and returned to ice. Following this, the cDNA was diluted in 20 μ l of RNase-free PCR water. 40 μ l of this diluted cDNA was then transferred into 0.5ml Eppendorf tubes and kept on ice. 2 μ l of this diluted cDNA was added to individual wells of an optical qPCR 96-well plate, followed by 8 μ l of the PCR mix. The qPCR plate was then thermosealed, centrifuged up to 1000rpm in the Grant bio LMC-3000, and loaded into the StepOnePlus real-time PCR system. The PCR reaction volume was 10 μ l, and 50 cycles

were performed within the standard 2-hour cycle.

References

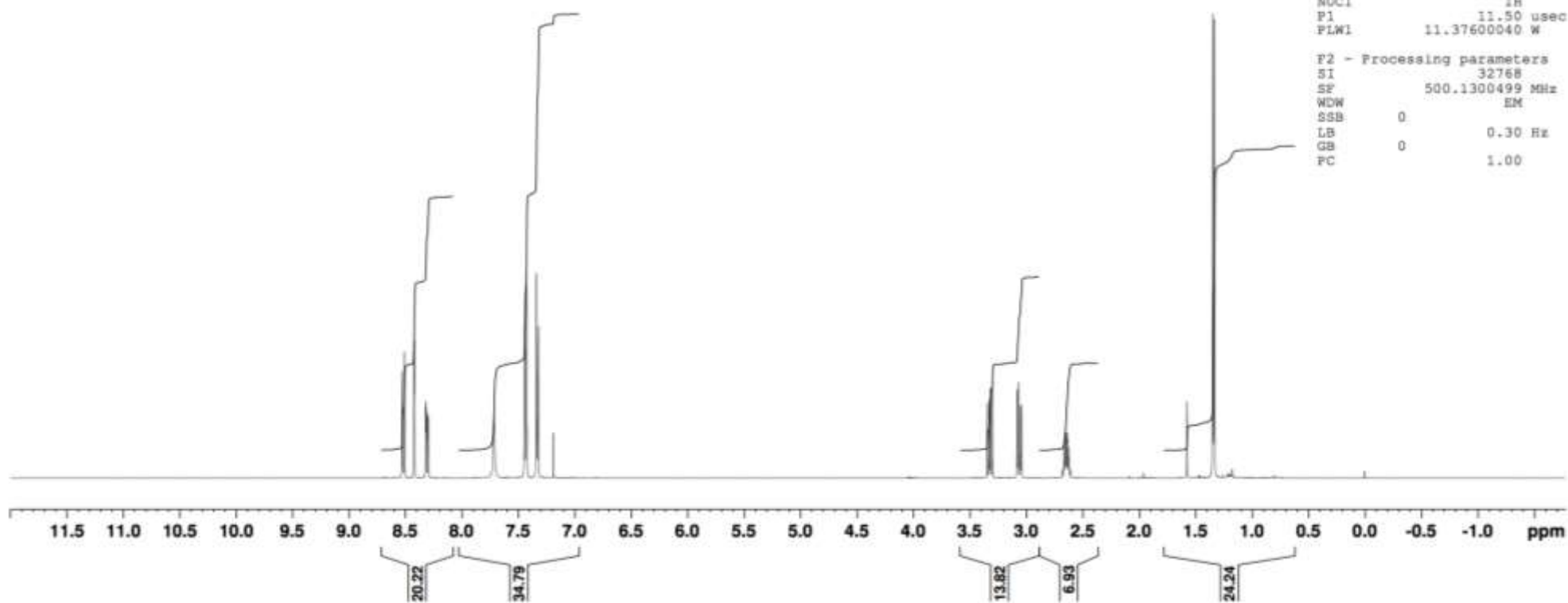
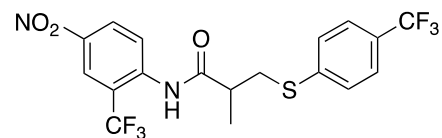
1. C. Chang, S. Lee, S. Yeh, T.M. Chang, Androgen receptor (AR) differential roles in hormone-related tumors including prostate, bladder, kidney, lung, breast and liver, *Oncogene*, 33 (2014) 3225-34.
2. P.E. Lonergan, D. J. Tindall, Androgen receptor signalling in prostate cancer development and progression. *J. Carcinogenesis*, 10 (2011) 20.
3. A.C. Pippione, D. Boschi, K. Pors, S. Oliaro-Bosso, M.L. Lolli. Androgen-AR axis in primary and metastatic prostate cancer: chasing steroidogenic enzymes for therapeutic intervention. *J. Cancer Metastasis Treat.* 3 (2017) 328-61.
4. G. Jenster, H.A. van der Korput, C. van Vroonhoven, T.H. van der Kwast, J. Trapman, A.O. Brinkmann, Domains of the human androgen receptor involved in steroid binding, transcriptional activation, and subcellular localization. *Mol. Endocrinol.* 5 (1991) 1396–1404.
5. G. Jenster, Coactivators and corepressors as mediators of nuclear receptor function: an update. *Mol. Cell. Endocrinol.* 143 (1998) 1–7.
6. A.O. Brinkmann, J. Trapman, Prostate cancer schemes for androgen escape. *Nat Med.* 6(6), (2000) 628-9.
7. A.O. Brinkmann, Molecular mechanisms of androgen action - a historical perspective. *Methods Mol Biol.* 776 (2011) 3-24.
8. C.D. Chen, D. S. Welsbie, C. Tran, S. H. Baek, R. Chen, R. Vessella, M.G. Rosenfeld, C.L. Sawyers, Molecular determinants of resistance to antiandrogen therapy. *Nat. Med.* 10 (2004) 33–39.
9. A.M. Moilanen, R. Riikonen, R. Oksala, L. Ravanti, E. Aho, G. Wohlfahrt, P.S. Nykänen, O.P. Törmäkangas, J.J. Palvimo, P.J. Kallio, Discovery of ODM-201, a new-generation androgen receptor inhibitor targeting resistance mechanisms to androgen signaling-directed prostate cancer therapies. *Sci. Rep.* 5 (2015) 12007.
10. P.A. Watson, V. K. Arora, C. L. Sawyers, Emerging Mechanisms of Resistance to Androgen Receptor Inhibitors in Prostate Cancer. *Nat. Rev. Cancer*, 15 (2015) 701–711.
11. P.L. McGinley, J. T. Koh, Circumventing Anti-Androgen Resistance by Molecular Design. *J. Am. Chem. Soc.* 129 (2007) 3822– 3823.
12. B. Fuqiang, D. Kush, L. Huifang, L. Eric, S.R. Paul, C. Artem, Best Practices of Computer-Aided Drug Discovery: Lessons Learned from the Development of a Preclinical Candidate for Prostate Cancer with a New Mechanism of Action, *J. Chem. Inf. Model.*, 57 (2017) 1018–1028.
13. S. Kandil, A.D. Westwell, C. McGuigan, 7-Substituted umbelliferone derivatives as androgen receptor antagonists for the potential treatment of prostate and breast cancer. *Bioorg Med Chem Lett.* 26(8), (2016) 2000-4.
14. D.A. Dart, S. Kandil, S. Tommasini-Ghelfi, G.S. de Almeida, C.L. Bevan, W. Jiang and A. D. Westwell, Novel trifluoromethylated enobosarm analogues with potent anti-androgenic activity *in vitro* and tissue selectivity *in vivo*, *Mol. Cancer. Ther.* 17(19) (2018) 1846.
15. S. Ferla, M. Bassetto, F. Pertusati, S. Kandil, A.D. Westwell, A. Brancale, C. McGuigan,

- Rational design and synthesis of novel anti-prostate cancer agents bearing a 3,5-bis-trifluoromethylphenyl moiety. *Bioorg Med Chem Lett.* 26(15) (2016) 3636-40.
16. Q. Shi, K. Wada, E. Ohkoshi, L. Lin, R. Huang, S.L. Morris-Natschke, M. Goto, K-H. Lee, Antitumor agents 290. Design, synthesis, and biological evaluation of new LNCaP and PC-3 cytotoxic curcumin analogs conjugated with anti-androgens. *Bioorg. Med. Chem.* 2012, 20, 4020-4031.
 17. M. Bassetto, S. Ferla, F. Pertusati, S. Kandil, A.D. Westwell, A. Brancale, C. McGuigan, Design and synthesis of novel bicalutamide and enzalutamide derivatives as antiproliferative agents for the treatment of prostate cancer. *Eur. J. Med. Chem.* 118 (2016) 230.
 18. B.B. Nandu, G.S. Dhananjay, R. Tarur, D. Raviraj, Synthesis of potential impurities of bicalutamide. *Synthetic Communications*, 39:9, (2009) 1516-1526.
 19. S. Tai, Y. Sun, J.M. Squires, H. Zhang, W.K. Oh, C.Z. Liang, PC3 is a cell line characteristic of prostatic small cell carcinoma. *Prostate*, 71 (2011) 1668-79.
 20. J. Kim, and G. A. Coetzee, Prostate specific antigen gene regulation by androgen receptor. *J. Cell. Biochem.* 93 (2004) 233-241.
 21. C. A. Heinlein, C. Chang, Androgen Receptor in Prostate Cancer, *Endocrine Reviews*, 25, 2 (2004), 276–308.
 22. J. S. Sack, K. F. Kish, C. Wang, R. M. Attar, S. E. Kiefer, Y. An, G.Y. Wu, J. E. Scheffler, M.E. Salvati, Jr.S.R. Krystek, R. Weinmann, H. M. Einspahr, Crystallographic structures of the ligand-binding domains of the androgen receptor and its T877A mutant complexed with the natural agonist dihydrotestosterone. *Proc. Natl. Acad. Sci. U.S.A.*, 98 (2001) 4904.
 23. C.E. Bohl, W. Gao, D.D. Miller, C.E. Bell, J.T. Dalton, Structural basis for antagonism and resistance of bicalutamide in prostate cancer. *Proc. Natl. Acad. Sci. U.S.A.*, 102 (2005) 6201.
 24. C.A. Marhefka, B.M. Moore, T.C. Bishop, L. Kirkovsky, A. Mukherjee, J.T. Dalton, D.
 25. D. Miller, Homology modeling using multiple molecular dynamics simulations and docking studies of the human androgen receptor ligand binding domain bound to testosterone and nonsteroidal ligands, *J. Med. Chem.*, 44 (2001) 1729-1740.
 26. K.P. Madauss, E.T. Grygielko, S.J. Deng, A. C. Sulpizio, T.B. Stanley, C. Wu, S.A. Short, S.K. Thompson, E.L. Stewart, N.J. Laping, S.P. Williams, J.D. Bray, A structural and in vitro characterization of asoprisnil: a selective progesterone receptor modulator. *Mol. Endocrinol.* 21 (2007) 1066.
 27. K. Pereira de Jesus-Tran, P.L. Cote, L. Cantin, J. Blanchet, F. Labrie, R. Breton, Comparison of crystal structures of human androgen receptor ligand-binding domain complexed with various agonists reveals molecular determinants responsible for binding affinity. *Protein Sci.*, 15 (2006) 987.
 28. M.D. Balbas, M.J. Evans, D.J. Hosfield, J. Wongvipat, V.K. Arora, P.A. Watson, C.L. Sawyers, Overcoming mutation-based resistance to antiandrogens with rational drug design. *eLife*, 2 (2013) e00499.

ACCEPTED MANUSCRIPT

¹H NMR spectrum of compound 25

25



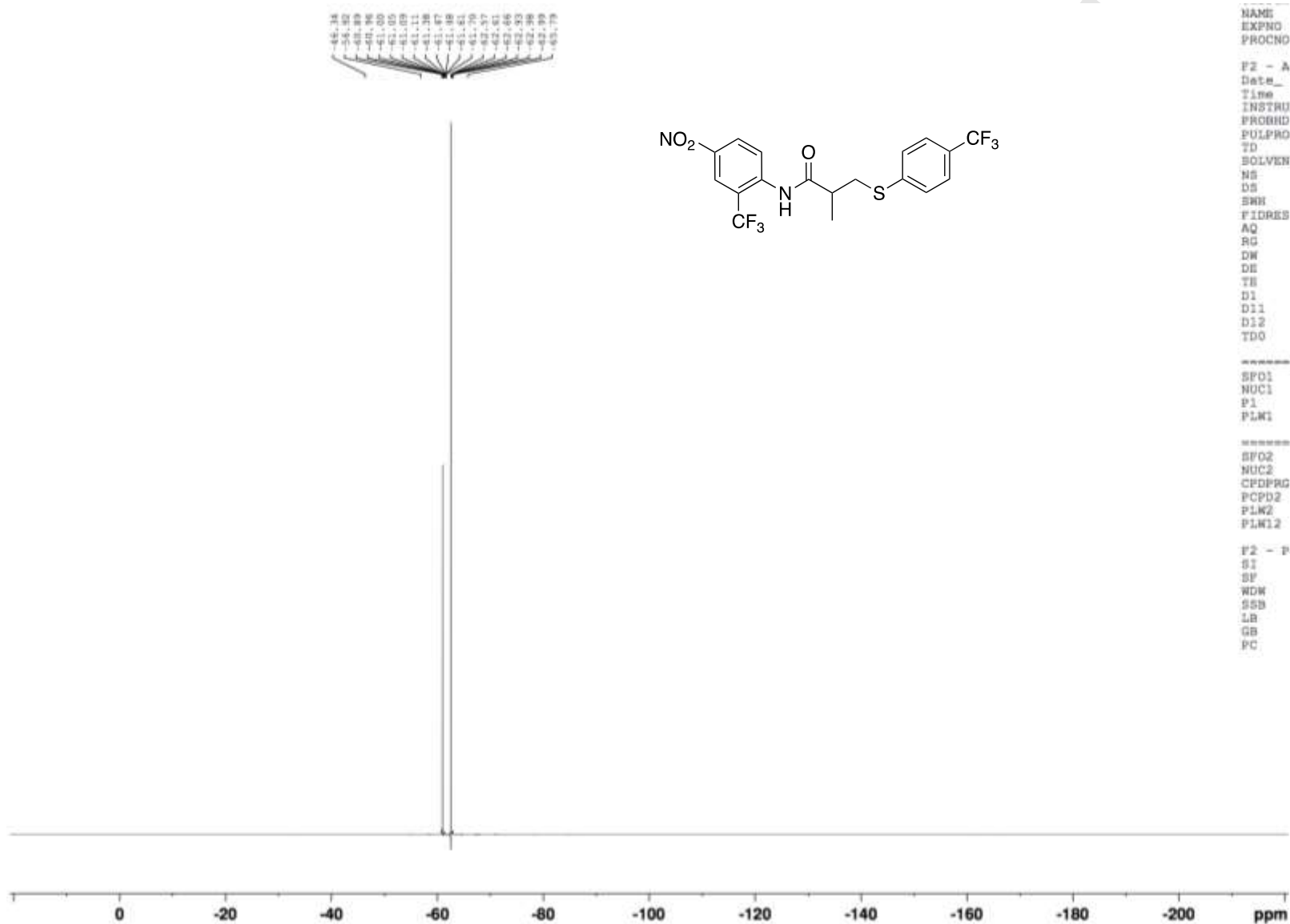
EXPNO 1
PROCNO 1

F2 - Acquisition Parameters
Date_ 20160915
Time 15.57
INSTRUM Avance500
PROBHD 5 mm QNP 1H/13
PULPROG zg30
TD 65536
SOLVENT CDCl3
NS 16
DS 2
SWH 10330.578 Hz
FIDRES 0.157632 Hz
AQ 3.1719425 sec
RG 181
DW 48.400 usec
DE 6.50 usec
TE 292.9 K
D1 1.00000000 sec
TD0 1

***** CHANNEL f1 *****
SFO1 500.1330885 MHz
NUC1 1H
P1 11.50 usec
PLW1 11.37600040 W

F2 - Processing parameters
SI 32768
SF 500.1300499 MHz
WDW EM
SSB 0
LB 0.30 Hz
GB 0
PC 1.00

¹⁹F NMR spectrum of compound 25



```

NAME          AW-SK-KL14
EXPNO         2
PROCNO        1

F2 - Acquisition Parameters
Date_         20160915
Time          15.59
INSTRUM       Avance500
PROBHD        5 mm QNP 1H/13
PULPROG       zgpg30
TD            131072
SOLVENT       CDCl3
NS            16
DS            4
SWH           113636.367 Hz
FIDRES        0.866977 Hz
AQ            0.5767168 sec
RG            575
DW            4.400 usec
DE            6.50 usec
TE            292.9 K
D1            1.00000000 sec
D11           0.03000000 sec
D12           0.00002000 sec
TD0           1

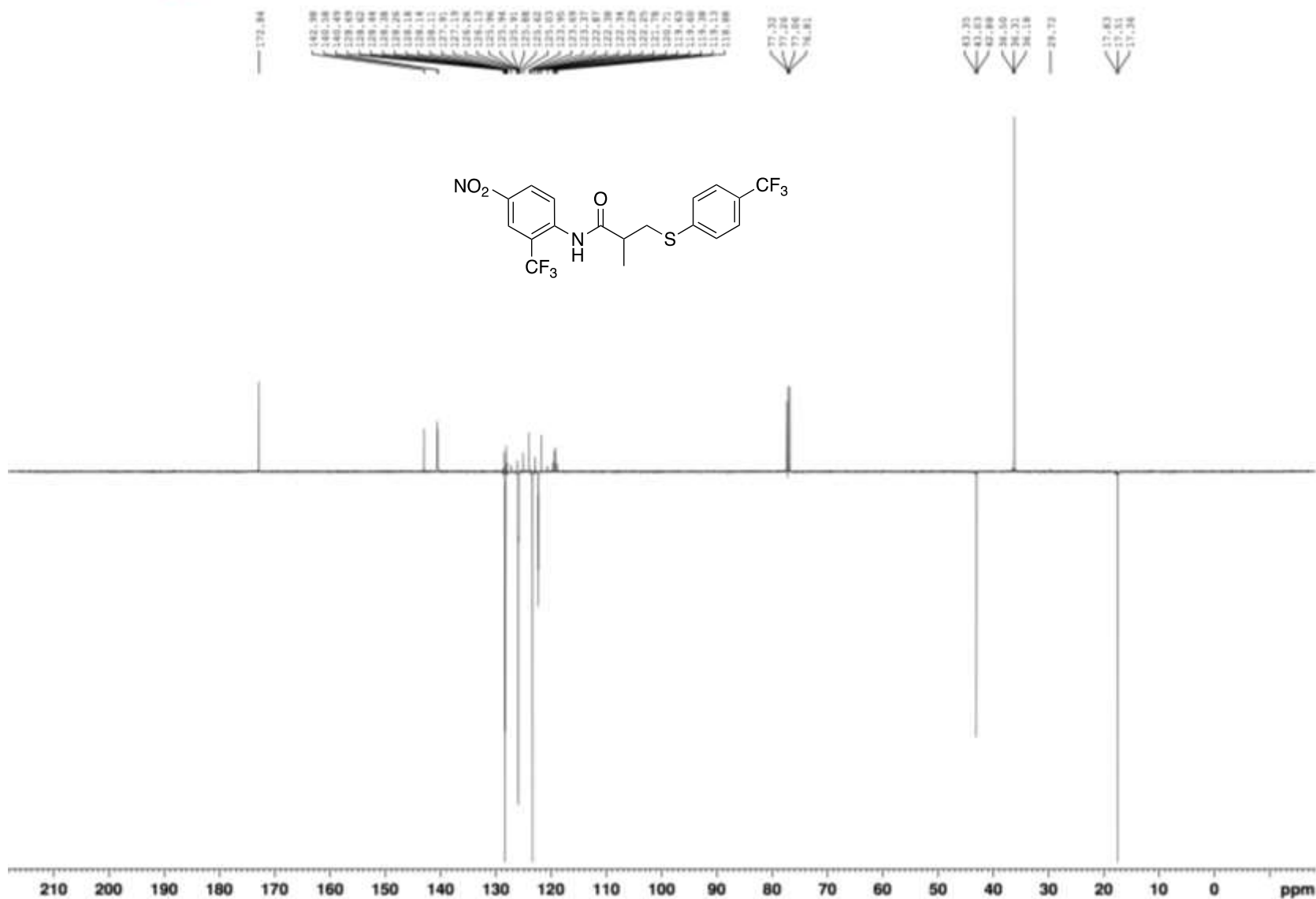
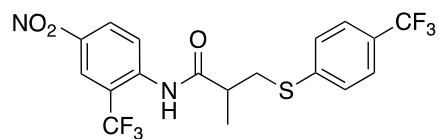
===== CHANNEL f1 =====
SFO1          470.5453182 MHz
NUC1           19F
P1            18.60 usec
PLW1          11.14099979 W

===== CHANNEL f2 =====
SFO2          500.1320005 MHz
NUC2           1H
PCPD2         waltz16
PCPD2         80.00 usec
PLW2          14.33199978 W
PLW12         0.29615000 W

F2 - Processing parameters
SI            65536
SF            470.5923772 MHz
WDW           EM
SSB           0
LB            0.30 Hz
GB            0
PC            1.40
    
```

¹³C NMR spectrum of compound 25

25



Current Data Parameters
NAME AW-SH-KL14
EXPNO 3
PROCNO 1

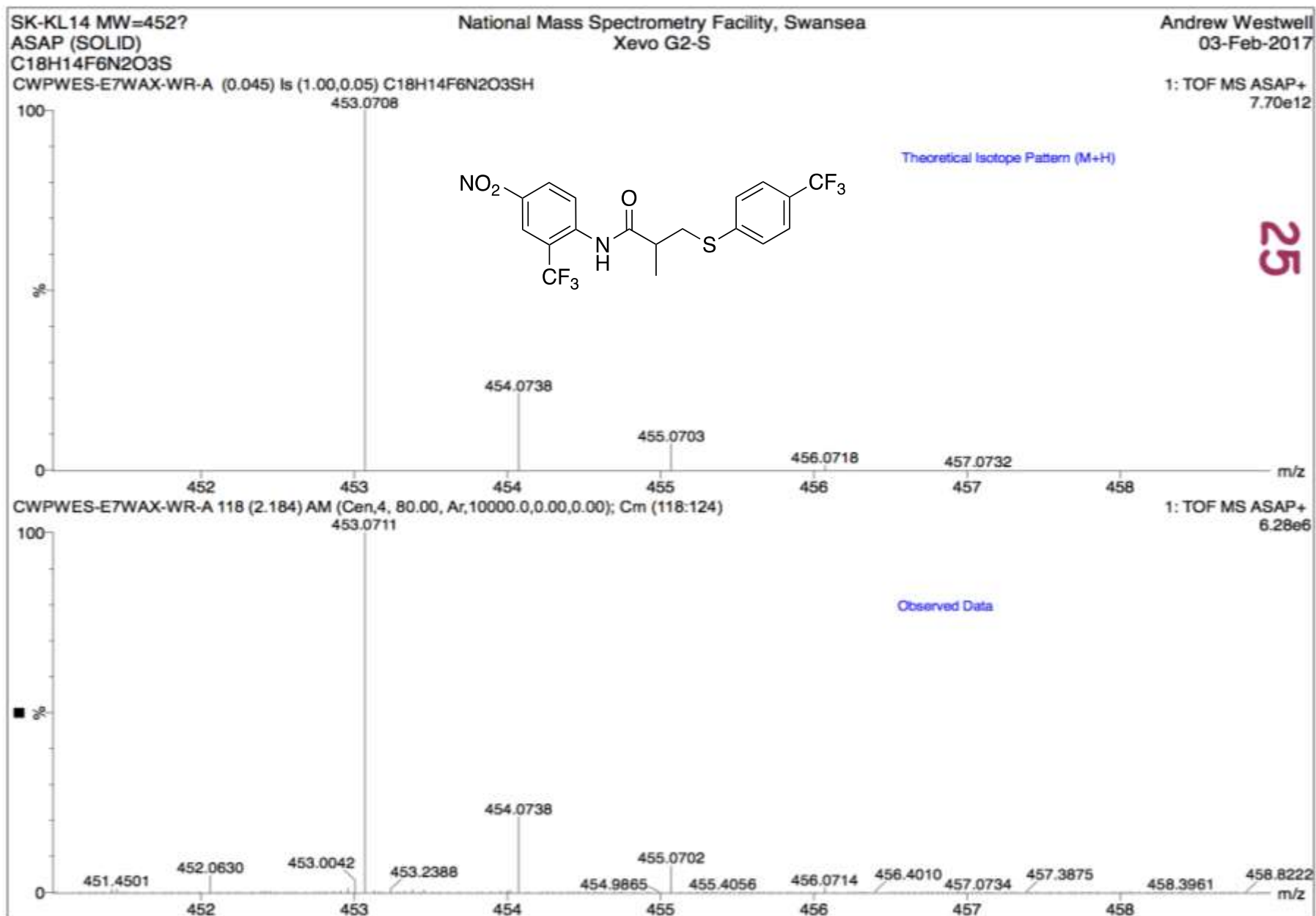
F2 - Acquisition Parameters
Date_ 20160915
Time 19.10
INSTRUM Avance500
PROBHD 5 mm QNP 1H/13
PULPROG pendant
TD 65536
SOLVENT CDCl3
NS 2360
DS 4
SWH 29761.904 Hz
FIDRES 0.454131 Hz
AQ 1.1010048 sec
RG 2050
DM 16.800 usec
DE 6.50 usec
TE 293.0 K
CHST2 145.0000000
D1 2.00000000 sec
D4 0.00172414 sec
D12 0.00002000 sec
D15 0.00431034 sec
D20 0.00345000 sec
TD0 20

===== CHANNEL f1 =====
SFO1 125.7703438 MHz
NUC1 13C
P1 7.20 usec
F2 14.40 usec
PLW1 101.27999878 W

===== CHANNEL f2 =====
SFO2 500.1320005 MHz
NUC2 1H
CPDPRG2 waltz16
P3 11.50 usec
P4 23.00 usec
PCPD2 60.00 usec
PLW2 14.33199978 W
PLW12 0.29615000 W

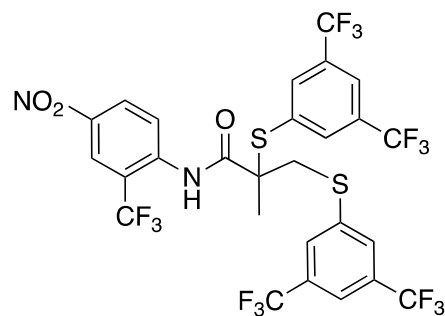
F2 - Processing parameters
SI 32768
SF 125.7577885 MHz
WDW EM
SSB 0
LB 1.00 Hz
GB 0
PC 1.40

Mass spectrum of compound 25



¹H NMR spectrum of compound 28

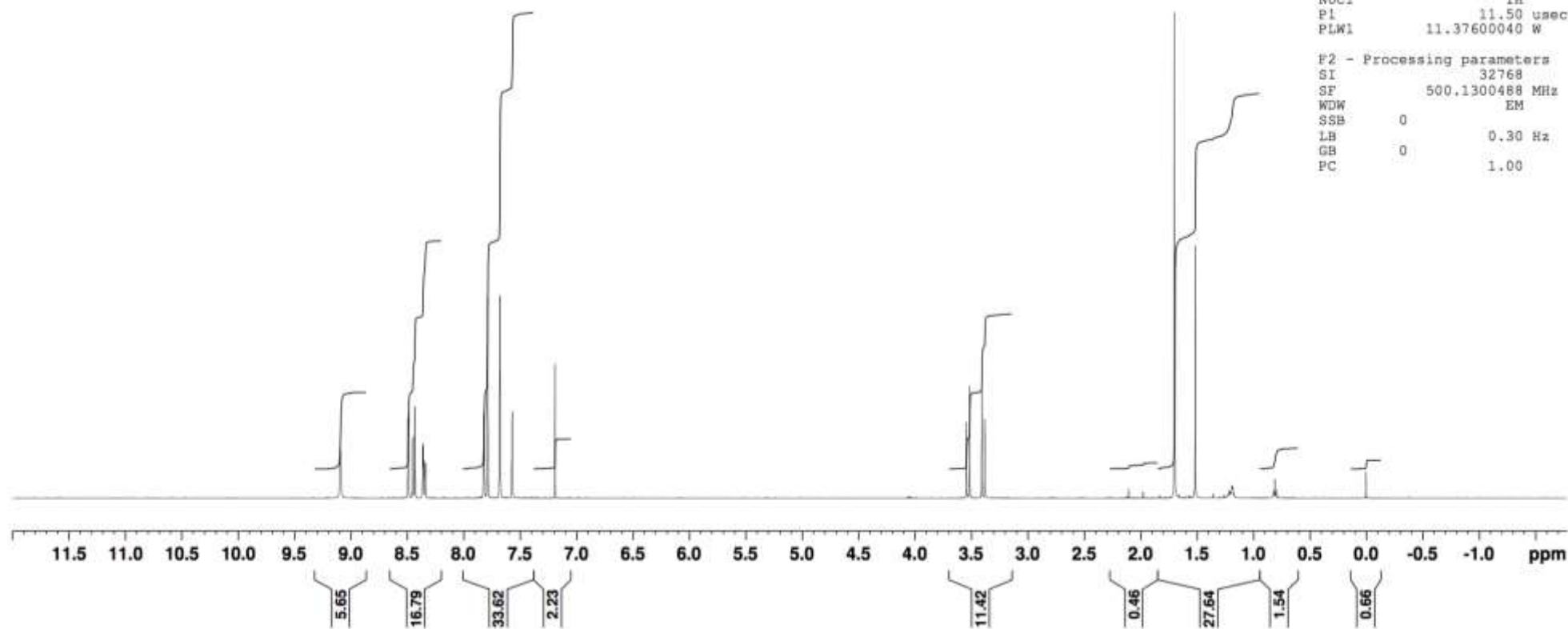
28



F2 - Acquisition Parameters
Date_ 20160915
Time 16.04
INSTRUM Avance500
PROBHD 5 mm QNP 1H/13
PULPROG zg30
TD 65536
SOLVENT CDCl3
NS 16
DS 2
SWH 10330.578 Hz
FIDRES 0.157632 Hz
AQ 3.1719425 sec
RG 362
DW 48.400 usec
DE 6.50 usec
TE 292.8 K
D1 1.00000000 sec
TD0 1

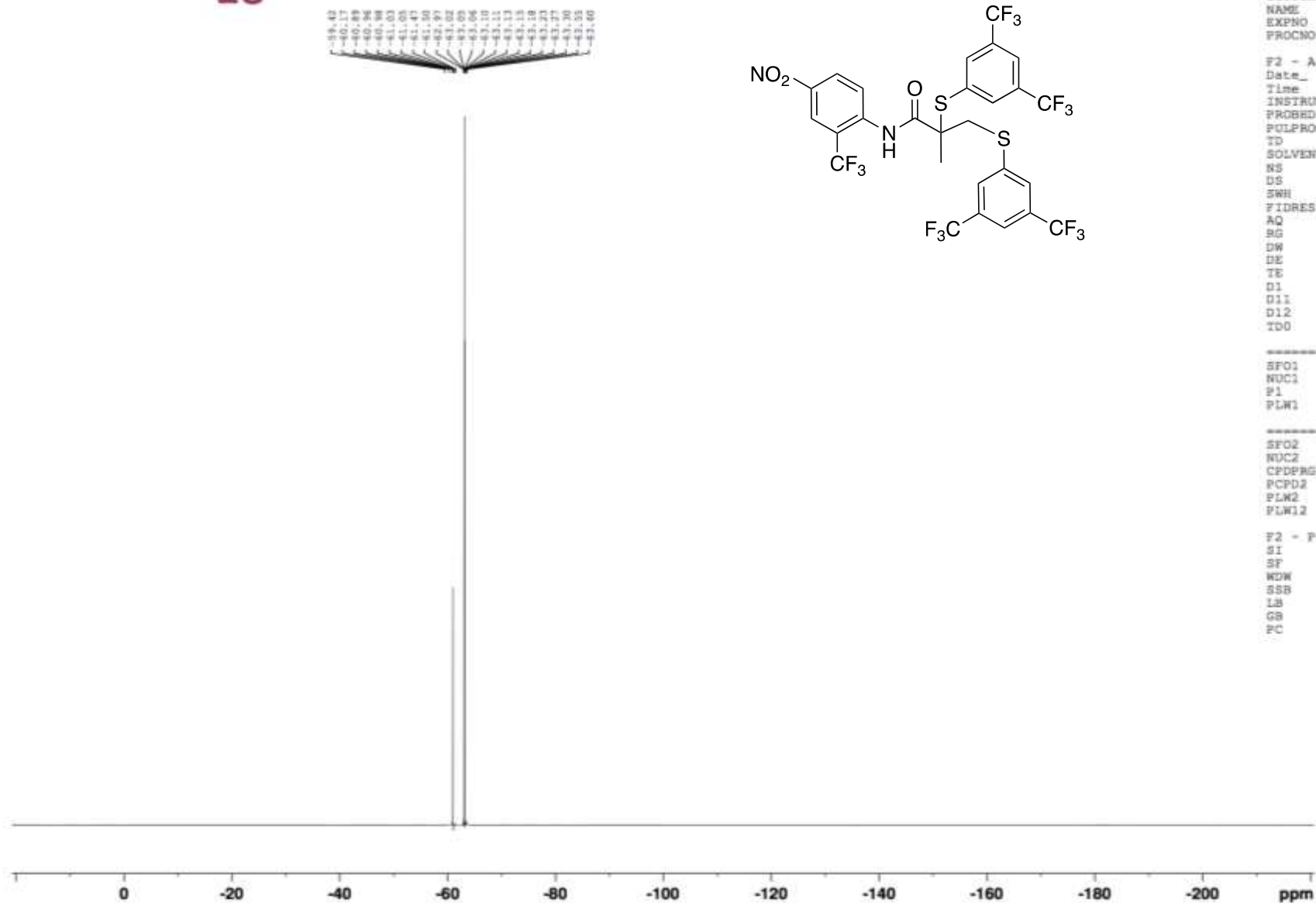
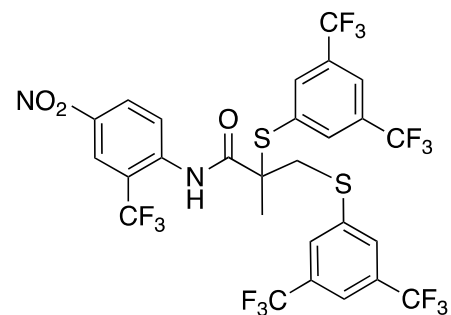
----- CHANNEL f1 -----
SFO1 500.1330885 MHz
NUC1 1H
P1 11.50 usec
PLW1 11.37600040 W

F2 - Processing parameters
SI 32768
SF 500.1300488 MHz
WDW EM
SSB 0
LB 0.30 Hz
GB 0
PC 1.00



¹⁹F NMR spectrum of compound 28

28



Current Data Parameters
NAME AW-SK-KL13-2
EXPNO 2
PROCNO 1

F2 - Acquisition Parameters
Date_ 20160915
Time 16.05
INSTRUM Avance500
PROBHD 5 mm QNP 1H/13
PULPROG zgpg30
TD 131072
SOLVENT CDCl3
NS 16
DS 4
SWH 113636.367 Hz
FIDRES 0.866977 Hz
AQ 0.5767168 sec
RG 1030
DW 4.400 usec
DE 6.50 usec
TE 292.9 K
D1 1.00000000 sec
D11 0.03000000 sec
D12 0.00002000 sec
TD0 1

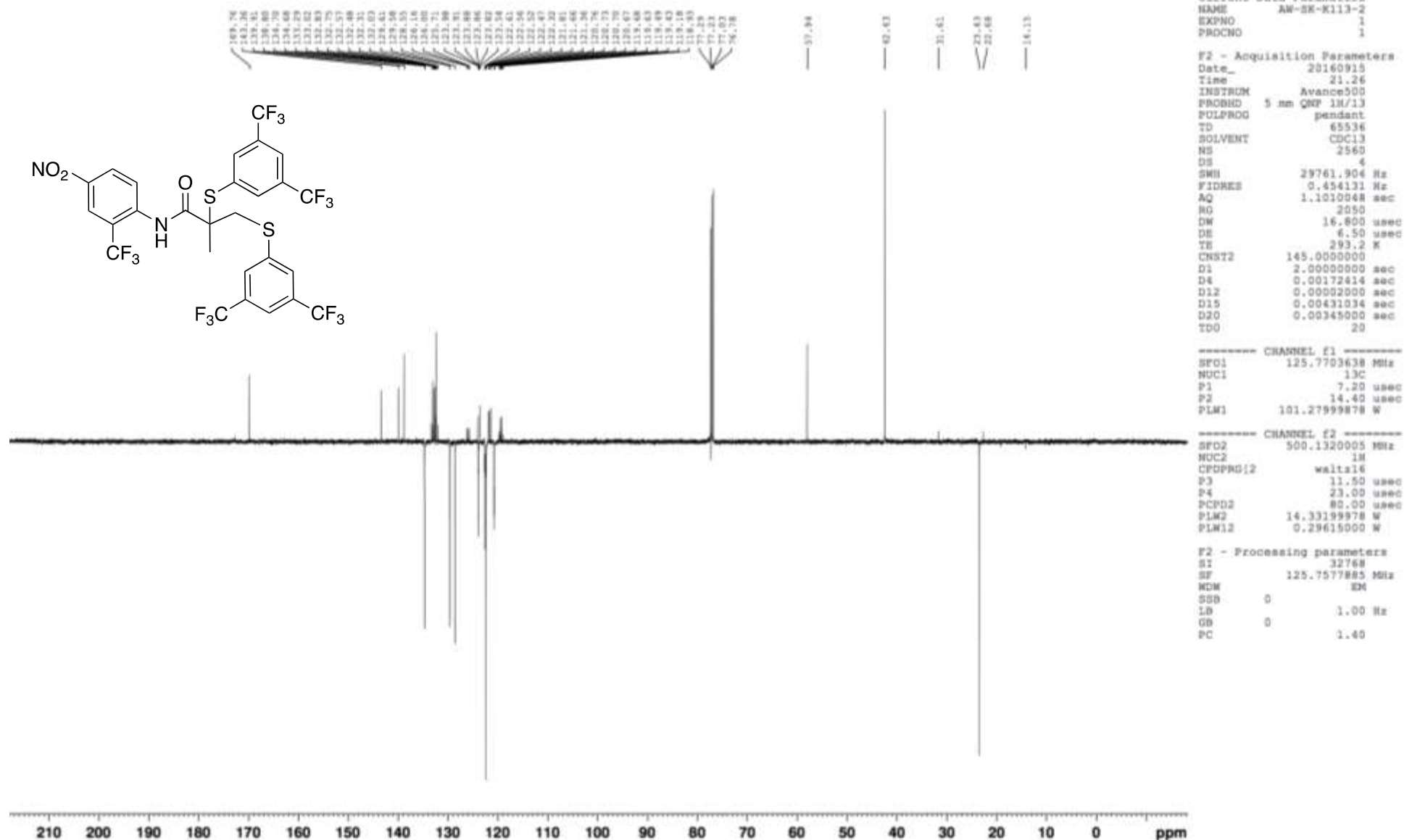
----- CHANNEL f1 -----
SFO1 470.5453182 MHz
NUC1 19F
P1 18.60 usec
PLW1 11.14099979 W

----- CHANNEL f2 -----
SFO2 500.1320005 MHz
NUC2 1H
PCPD2 waltz16
PCPD2 80.00 usec
PLW2 14.33199978 W
PLW12 0.29615000 W

F2 - Processing parameters
SI 65536
SF 470.5923772 MHz
WDW EM
SSB 0
LB 0.30 Hz
GB 0
PC 1.40

¹³C NMR spectrum of compound 28

28



Mass spectrum of compound 28

SK-KL 13-2 MW=732?

ASAP(MeOH)

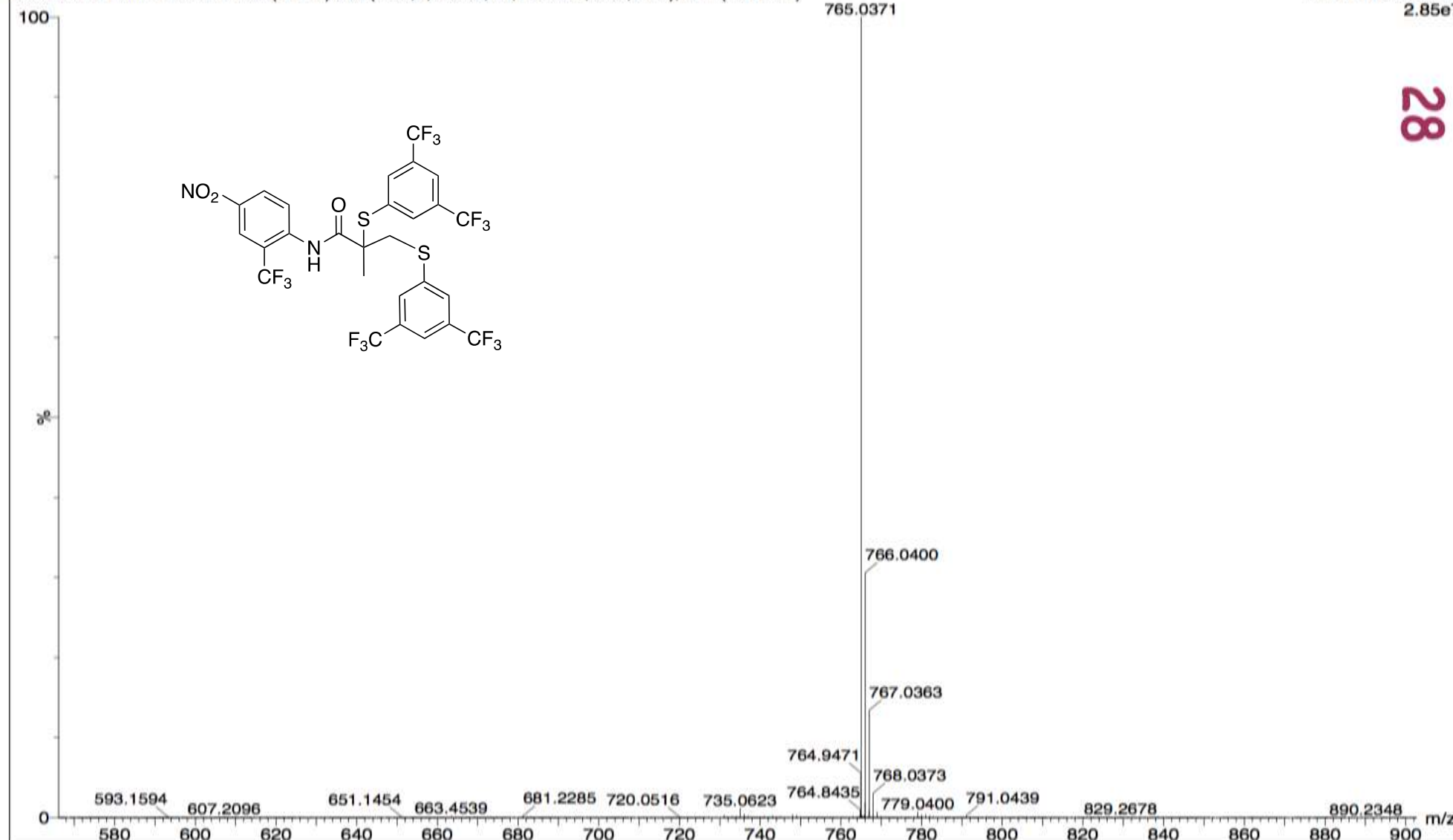
C₂₇H₁₅F₁₅N₂O₃S

CWPWES-E4TRX-WG-A 288 (2.670) AM (Cen,4, 80.00, Ar,10000.0,0.00,0.00); Cm (281:316)

National Mass Spectrometry Facility, Swansea
Xevo G2-S

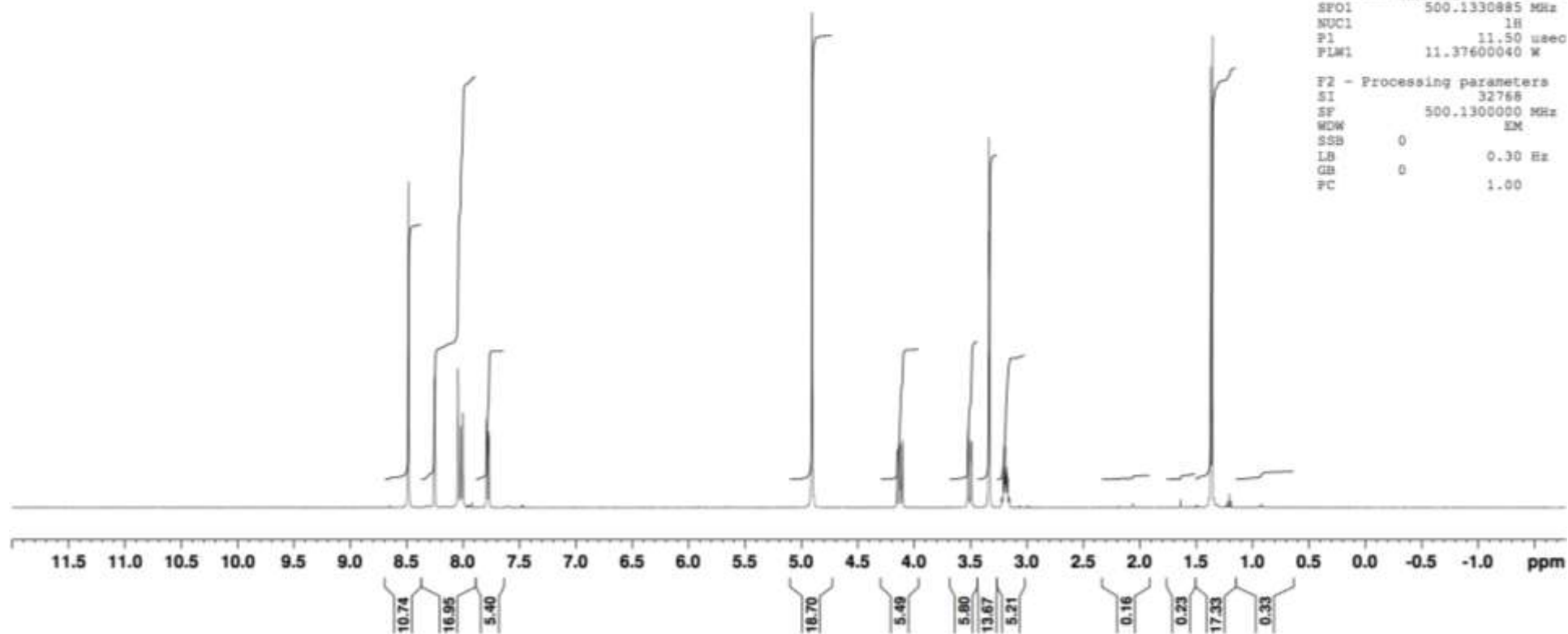
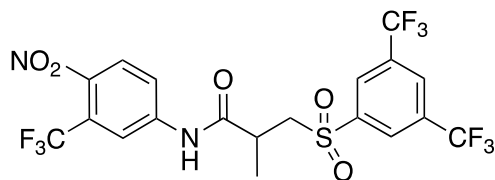
Amdrew
25-Oct-2016

1: TOF MS ASAP+
2.85e7



¹H NMR spectrum of compound 35

35



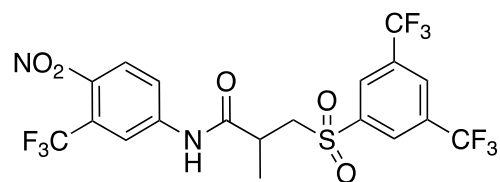
```
PROCNO 1
F2 - Acquisition Parameters
Date_ 20160708
Time 13.35
INSTRUM Avance500
PROBHD 5 mm QNP 1H/13
PULPROG zg30
TD 65536
SOLVENT MeOD
NS 16
DS 2
SWH 10330.578 Hz
FIDRES 0.157632 Hz
AQ 3.1719425 sec
RG 406
DW 48.400 usec
DE 6.50 usec
TE 295.0 K
D1 1.00000000 sec
TD0 1

===== CHANNEL f1 =====
SFO1 500.1330885 MHz
NUC1 1H
P1 11.50 usec
PLW1 11.37600040 W

F2 - Processing parameters
SI 32768
SF 500.1300000 MHz
WDW EM
SSB 0
LB 0.30 Hz
GB 0
PC 1.00
```

¹⁹F NMR spectrum of compound 35

35



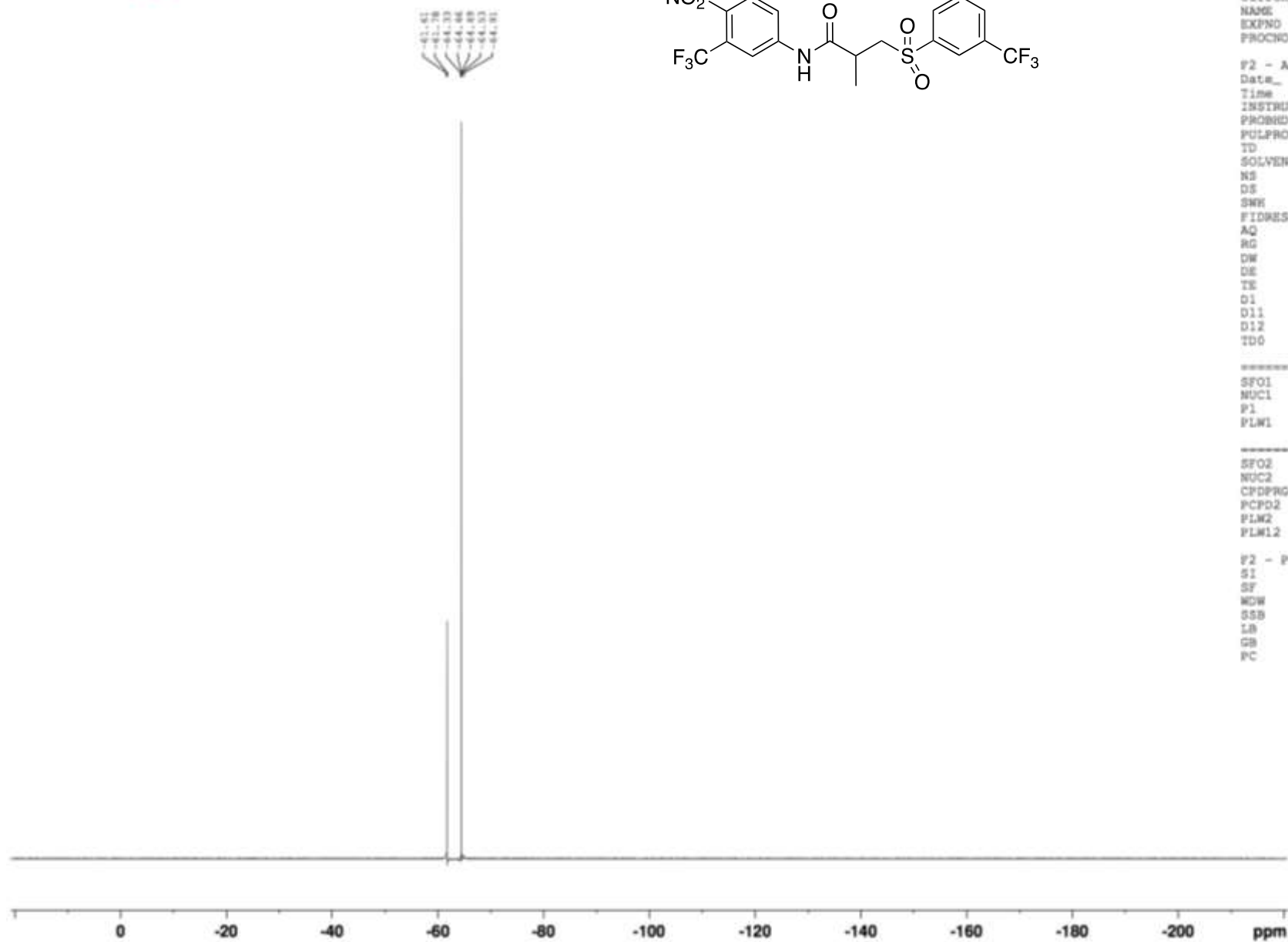
Current Data Parameters
NAME AM-SK-KL4
EXPNO 2
PROCNO 1

F2 - Acquisition Parameters
Date_ 20160708
Time 13.38
INSTRUM Avance500
PROBHD 5 mm QNP 1H/13
PULPROG zgpg30
TD 131072
SOLVENT MeOD
NS 16
DS 4
SWH 113636.367 Hz
FIDRES 0.866977 Hz
AQ 0.5767168 sec
RG 2050
DW 4.400 usec
DE 6.50 usec
TE 295.0 K
D1 1.00000000 sec
D11 0.03000000 sec
D12 0.00002000 sec
TD0 1

===== CHANNEL f1 =====
SFO1 470.5453182 MHz
NUC1 19F
P1 18.60 usec
PLW1 11.14099979 W

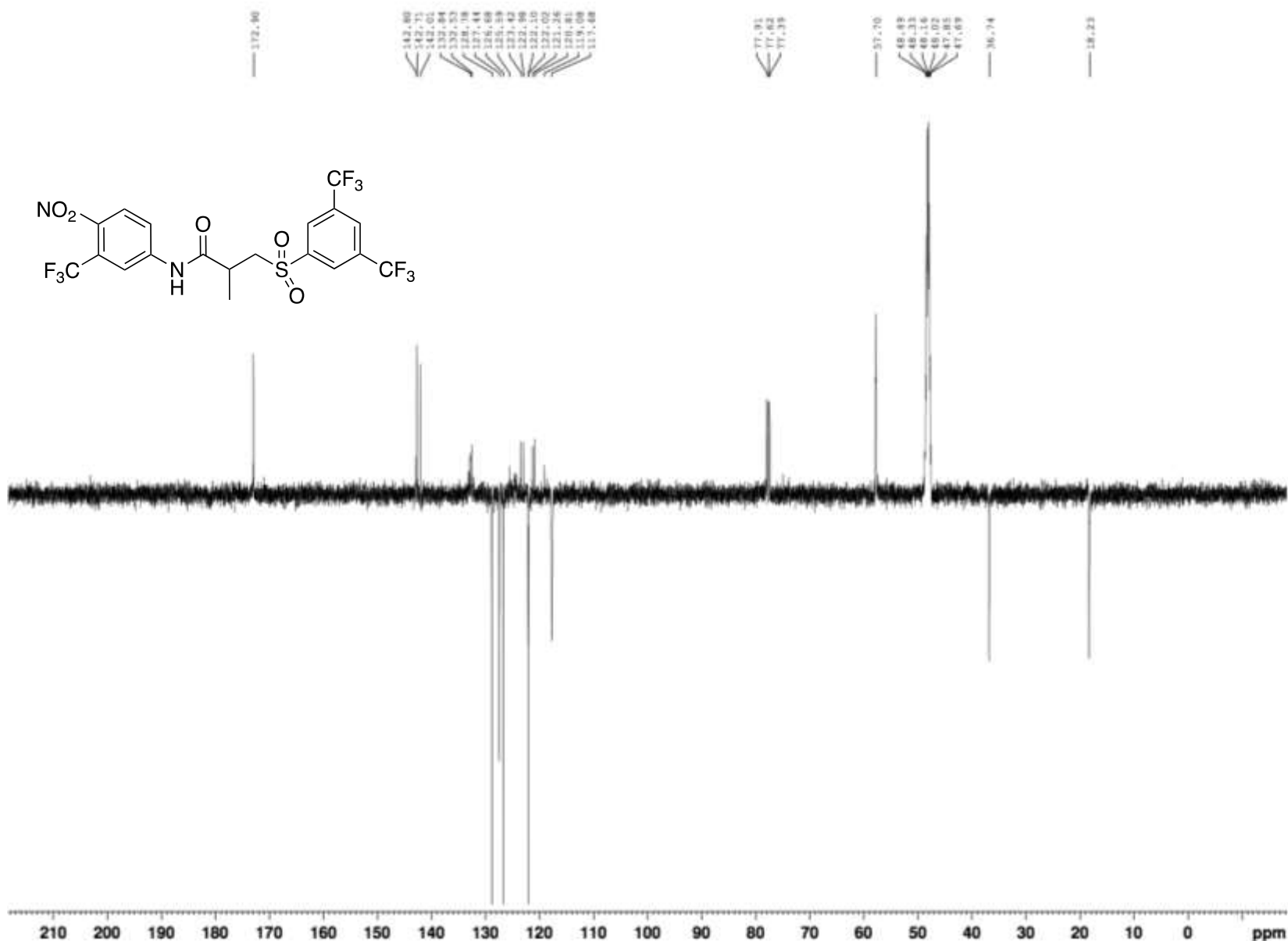
===== CHANNEL f2 =====
SFO2 500.1320005 MHz
NUC2 1H
PCPD2 waltz16
PCPD2 80.00 usec
PLW2 14.33199978 W
PLW12 0.29615000 W

F2 - Processing parameters
SI 65536
SF 470.5923772 MHz
WDW EM
SSB 0
LB 0.30 Hz
GB 0
PC 1.40



¹³C NMR spectrum of compound 35

35



Current Data Parameters
NAME AM-SK-KL4
EXPNO 4
PROCNO 1

F2 - Acquisition Parameters
Date_ 20160720
Time 23.32
INSTRUM Avance500
PROBHD 5 mm QNP 1H/13
PULPROG pendant
TD 65536
SOLVENT MeOD
NS 2304
DS 4
SWH 29761.904 Hz
FIDRES 0.454131 Hz
AQ 1.1010048 sec
RG 2050
DW 16.800 usec
DE 6.50 usec
TE 295.4 K
CNS12 145.0000000
D1 2.00000000 sec
D4 0.00172414 sec
D12 0.00002000 sec
D15 0.00431034 sec
D20 0.00345000 sec
TD0 18

===== CHANNEL f1 =====
SFO1 125.7703638 MHz
NUC1 13C
P1 7.20 usec
P2 14.40 usec
PLW1 101.27999878 W

===== CHANNEL f2 =====
SFO2 500.1320005 MHz
NUC2 1H
CPDPRG2 waltz16
P3 11.50 usec
P4 23.00 usec
PCPD2 80.00 usec
PLW2 14.33199978 W
PLW12 0.29615000 W

F2 - Processing parameters
S1 32768
SF 125.7577885 MHz
WDW EM
SSB 0
LB 1.00 Hz
GB 0
PC 1.40

Mass spectrum of compound 35

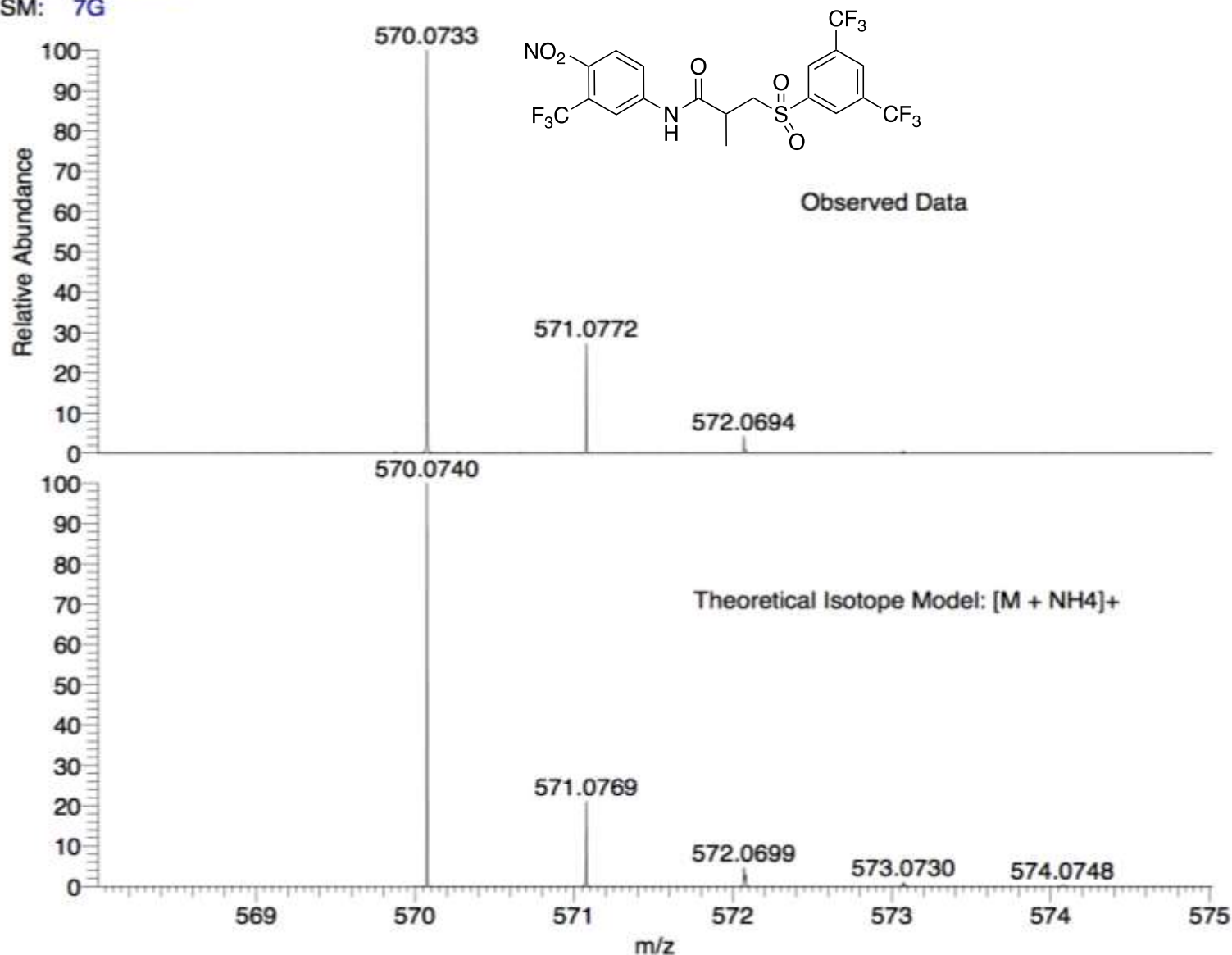
SK-KL4
(MeOH)/MeOH + NH₄OAc
C₁₉H₁₃F₉N₂O₅S

EPSRC National Facility Swansea
LTQ Orbitrap XL

CWPWES
03/08/2016 07:11:30

SM: 7G

NL:
4.21E6
CWPWES_IMNS1_58#32-45
RT: 0.72-1.02 AV: 12 T: FTMS
+ p NSI Full ms
[120.00-1935.00]



NL:
1.77E4
C₁₉H₁₃F₉N₂O₅SNH₄:
C₁₉H₁₇F₉N₃O₅S₁
p (gss, s /p:40) Chrg 1
R: 100000 Res .Pwr . @FWHM